
KVCOMM: Online Cross-context KV-cache Communication for Efficient LLM-based Multi-agent Systems

Hancheng Ye¹, Zhengqi Gao², Mingyuan Ma¹,
 Qinsi Wang¹, Yuzhe Fu¹, Ming-Yu Chung¹, Yueqian Lin¹,
 Zhijian Liu³, Jianyi Zhang¹, Danyang Zhuo¹, Yiran Chen¹

¹Duke University, ²MIT, ³NVIDIA
 hancheng.ye@duke.edu

Abstract

Multi-agent large language model (LLM) systems are increasingly adopted for complex language processing tasks that require communication and coordination among agents. However, these systems often suffer substantial overhead from repeated reprocessing of overlapping contexts across agents. In typical pipelines, once an agent receives a message from its predecessor, the full context—including prior turns—must be reprocessed from scratch, leading to inefficient processing. While key-value (KV) caching is an effective solution for avoiding redundant computation in single-agent settings where prefixes remain unchanged, it cannot be directly reused in multi-agent scenarios due to diverging prefixes introduced by agent-specific context extensions. We identify that the core challenge lies in the *offset variance* of KV-caches across agents. To address this, we propose KVCOMM, a training-free framework that enables efficient prefilling in multi-agent inference by reusing KV-caches and aligning cache offsets of overlapping contexts under diverse prefix contexts. KVCOMM estimates and adjusts KV-caches for shared content by referencing a pool of cached examples—termed *anchors*—that store observed cache deviations under varying prefixes. The anchor pool is maintained and updated online, allowing dynamic adaptation to distinct user requests and context structures. KVCOMM achieves over 70% reuse rate across diverse multi-agent workloads, including retrieval-augmented generation, math reasoning, and collaborative coding tasks, all without quality degradation. Particularly, when each fully-connected agent receives 1K input tokens with 512 prefix tokens and 512 output tokens under a five-agent setting, KVCOMM achieves up to 7.8× speedup compared to the standard prefill pipeline, reducing TTFT from ∼430ms to ∼55ms. Code is available at <https://github.com/FastMAS/KVCOMM>.

1 Introduction

Large Language Models (LLMs) such as GPT-4o [1] and Llama-3 [11] have triggered a surge of interest in collaborative multi-agent systems, where several specialized agents exchange messages to collaboratively solve complex tasks such as retrieval-augmented question answering, mathematical reasoning, and tool-augmented program synthesis [63, 9, 51, 38, 49, 60, 54, 18]. In these settings, every message processed by LLM agents must first go through the prefill stage prior to decoding, during which the model encodes the full conversation history and constructs *key-value (KV) caches*. Although multiple agents often share overlapping context (*e.g.*, retrieved passages or peer outputs), they always redundantly recompute KV-caches for all input tokens, resulting in significant inefficiency of prefilling computation [27, 56, 30], which is defined as a *multi-context redundancy* issue in the

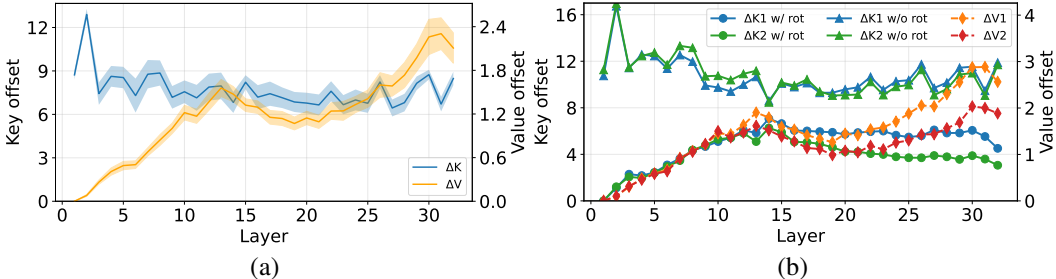


Figure 1: (a) Mean KV-cache offset (measured by ℓ_2 norm) from the base-context cache for the *same token* across ten distinct prefixes. Shaded regions indicate standard deviation across these prefixes. (b) KV-cache offset comparison between two embedding-similar tokens from the base-context caches when both tokens are prefixed with a new context. “ $\Delta K1$ w/ rot” and “ $\Delta K2$ w/ rot” represent Key offsets of two tokens with position alignment, respectively. “ $\Delta K1$ w/o rot” and “ $\Delta K2$ w/o rot” refer to Key offsets without alignment. “ $\Delta V1$ ” and “ $\Delta V2$ ” denote Value offsets of two tokens.

multi-agent system. For example, a single 8B Llama needs ~ 430 ms to prefill a 3K-token prompt on one H100 GPU. If each of M agents receives messages from all of its peers, the total prefilling complexity of these repeated computations scales as $\mathcal{O}(M^2)$, posing inefficiency in the utilization of computation and a major challenge for real-time multi-agent collaboration.

Recent works attempt to reduce prefilling overhead primarily through four techniques: prompt-level reuse [10], selective recomputation [58, 27, 56], cache compression [28], kernel-level optimizations [67, 46]. While effective in their target scenarios, these methods share a *fixed* acceleration policy crafted for a particular workload. However, our empirical study reveals that the same shared text can incur vastly different KV deviations once it is preceded by different prefix contexts, *e.g.*, system messages with different roles or upstream agents with different output lengths (see Figure 1a). When the acceleration policy fails to model such an *offset-variance* problem, cache reuse becomes misaligned, causing either large accuracy drops or a fallback to full recomputation that erodes the speed benefits.

This observation motivates a **prompt-adaptive** paradigm that (i) dynamically determines how to reuse KV-caches at *runtime* for each incoming prompt given diverse prefix contexts, and (ii) requires no additional training, profiling, or model modifications, allowing easy adoption on various tasks and agent workloads. To our knowledge, no existing method simultaneously satisfies both desiderata.

In this paper, we introduce *training-free online KV-cache communication* (KVCOMM), a drop-in framework that accelerates multi-agent systems through *shared-context reuse with adaptive KV offsetting*. The key insight is to treat every reuse attempt as an *approximate translation* problem, where the KV-cache of overlapping text becomes reusable for a new prefix once the positional shift and cache offsets from similar samples are identified. As illustrated in Figure 1b, the KV-cache offsets of two similar tokens prefixed with two different prompts present similar distributions across layers, where the deviation of the rotated Key cache is significantly smaller than the unrotated one. Therefore, KVCOMM proposes an **anchor pool** of previously shared samples along with their measured offsets under diverse prefixes. At inference time, the framework first locates the nearest anchor(s) for the requested segment via token similarity (**Anchor Matching**) and then predicts the offset by interpolating their stored deviations, avoiding a replay through the prefilling stage (**Offset Approximation**). For the Key cache update, the cache will first be encoded to the correct position and then biased by the estimated offset, while for the Value cache update, since it has no positional information, the offset is directly added to the cache. Meanwhile, the anchor pool is updated online to catch up with the new input distribution. That is, once the cache of an input segment is predicted as unshareable, it will be marked as an anchor and measure the cache offset under each prefix to extend the reusing range for the subsequent input samples. For the least matched anchors, they would be periodically freed up to save memory consumption and computation cost.

In summary, KVCOMM represents a substantial advancement in adaptively efficient KV-cache sharing in the LLM-based multi-agent system without training or recomputation, offering a practical path toward efficient agent communication. The main contribution is threefold:

- We identify the *multi-context redundancy* as a key challenge for efficient prefilling in the multi-agent scenario, and characterize the *offset-variance problem* that limits traditional KV sharing in such a setting, which to our knowledge, has not been covered by prior work.
- We propose KVCOMM, the first *training-free, prompt-adaptive* cache-sharing framework for efficient prefilling of multi-agent systems, requiring only a few anchors to effectively

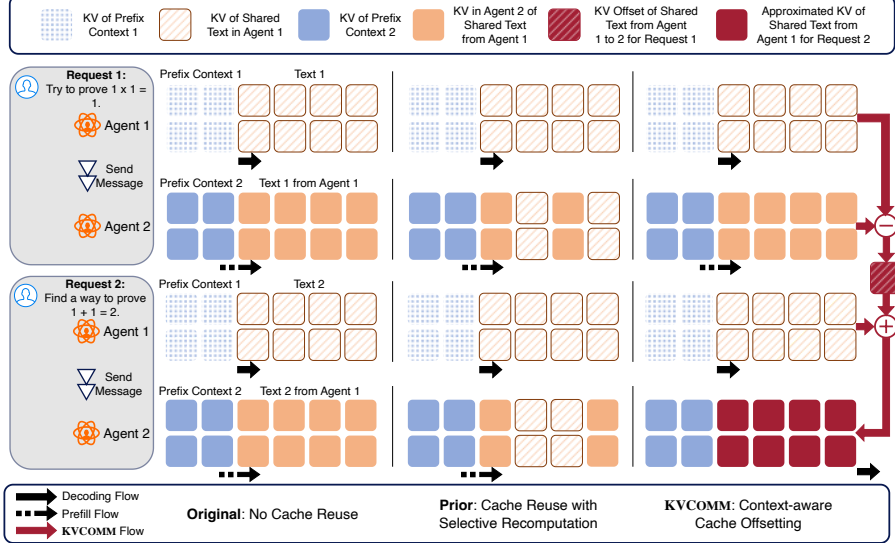


Figure 2: Comparisons with existing KV-cache reuse methods. (Left) The original no-cache-reuse baseline method densely prefills the tokens of all requests. (Middle) Selective recomputation methods [58, 27] select the most critical part of KV-cache for recomputation and reuse the remaining cache of each request. (Right) KVCOMM reuses all KV-caches of the shared context and introduces context-aware cache offsets to align with different prefix contexts, where the context-aware offset refers to the KV-cache deviation induced by the changed prefix context. Such an offset is approximated by the ground-truth ones of previous similar requests. After approximation, the model runner directly starts decoding without prefill.

approximate KV-cache offsets across different prefix. In KVCOMM, an efficient KV-cache management system is designed to support fast anchor lookup.

- Extensive experiments on three representative tasks with different models, including retrieval augmented generation (RAG), math reasoning, and programming, demonstrate that KVCOMM can achieve $\sim 6.7 \times$ average prefill speed-up where each agent is deployed by Llama-3.1-8B-instruct [11] on an NVIDIA H100 GPU. Meanwhile, as the reuse rate reaches 95% across 1,319 samples in a four-agent system for GSM8K [7], KVCOMM achieves comparable performance to the original workload (less than 2.5% accuracy drop).

2 Related Work

2.1 LLM-Based Multi-Agent Systems

The idea of distributing a complex task across multiple specialized LLM agents has rapidly progressed, from early frameworks such as AutoGPT [35] to mature tool-augmented systems for retrieval, coding, and robotics [17, 26, 39, 63, 9, 48, 22, 50, 51, 62, 55, 3, 31, 52, 24, 15, 42, 19, 40, 23]. Recent studies propose curriculum fine-tuning to promote role specialization [66], graph-structured message routing [57, 69], and hierarchical decision making [32]. Yet practically, each agent still performs a full **prefill** pass for every turn, recomputing the KV tensors over large shared contexts. As agent graphs grow wider or deeper, the prefill complexity of these repeated computations scales quadratically, posing inefficiency in computation utilization. Addressing the prefill bottleneck is thus a prerequisite for scaling multi-agent LLM applications to real-time settings.

2.2 KV-cache Acceleration and Reuse

KV-cache Sharing Scenario. Prior research has identified three principal patterns for reusing the KV-cache in transformers. (i) *Multi-request sharing* exploits identical prefixes across requests from different users; by copying the KV-cache of the shared prefix, servers can bypass most of the prefill compute when only the tail differs. (ii) *Multi-turn sharing* keeps the cache alive throughout the turns of a single conversation, thus avoiding recomputation of the history. (iii) *Multi-context sharing* handles inputs whose overlapping segment appears at *different contexts*, which aims to filter out the impact of the prefixed prompt in the KV-cache and to combine current context information into the reused KV-cache. Most of these techniques assume that *every agent runs the same model architecture*—typically a vanilla RoPE-based decoder—so that a cached key can be translated by a simple rotation without re-encoding [37, 47]. DroidSpeak [27] extends the sharing from the base model to the fine-tuned one by profiling which layers remain shareable. Current industrial serving

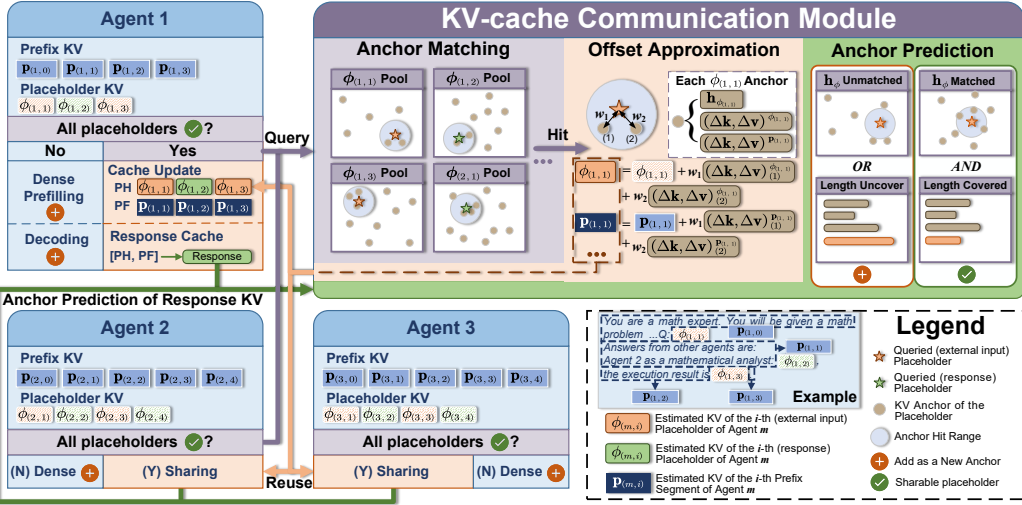


Figure 3: Overview of the KVCOMM framework in a three-agent scenario. Initially, each agent precomputes and stores the KV-cache of prefix segments from its prompt template for future reuse. At runtime, upon receiving a new request, agents check placeholder shareability and query matched anchors. Matched anchors help approximate KV-cache offsets for placeholders and subsequent prefixes through embedding-based interpolation. The matching criteria consider length compatibility and embedding proximity. The updated KV-caches are concatenated for efficient decoding. After decoding, the KV-cache Communication module assesses newly generated caches for potential sharing with other agents based on the established matching rules.

stacks [21, 68, 5] expose the same constraint that architectural identity is a prerequisite for cache reuse.

Existing methods on KV-cache acceleration primarily explore four paradigms. (1) *Prompt-Level Reuse* [10]. PromptCache [10] introduces Prompt Markup Language to explicitly define reusable text segments whose KV-caches are precomputed offline and directly fetched at inference, eliminating recomputation but restricted to fixed prompt structures. (2) *Selective Recomputation* [58, 27, 56]. CacheBlend [58] dynamically identifies and updates tokens exhibiting high variance in KV-caches. DroidSpeak [27] leverages profiling to identify critical attention layers whose KV-caches must be refreshed to maintain accuracy. KVLink [56] further extends it by fine-tuning special tokens and adjusting positional embeddings, enabling KV reuse across multiple document contexts. (3) *Cache Compression* [28]. CacheGen [28] compresses KV-caches into adaptive bit-streams based on available bandwidth; however, the entire token sequence still undergoes compression computations, limiting latency improvements. (4) *Kernel-Level Optimizations* [67, 46]. PrePacking [67] employs a bin-packing strategy to batch variable-length prompts into unified sequences. LoongServe [46] designs Elastic Sequence Parallelism to dynamically manage parallelism strategies and overlap cache migration with decoding steps to enhance GPU utilization. Figure 2 compares the main difference between KVCOMM and existing KV-cache sharing methods. Generally, KVCOMM explores a completely novel paradigm that can reuse all shareable KV-caches regardless of diverse prefix contexts, and align them by leveraging the context-aware cache offsets observed in previous samples.

3 Proposed Approach

3.1 Preliminaries

Large Language Models and KV-cache. Let $\mathbf{x} = [\mathbf{h}^1, \dots, \mathbf{h}^L]$ denote a list of token embedding sequences, with $\mathbf{h}^l \in \mathbb{R}^{N \times D}$ representing the input token embedding of the l -th transformer layer, where N is the number of tokens and D is the feature dimension. For \mathbf{h}_n^l (where $n = 1, 2, \dots, N$), it is projected by the l -th transformer layer to Query, Key, and Value vectors for the subsequent attention computation using: $\mathbf{q}_n^l = R_n W_Q^l \mathbf{h}_n^l$, $\mathbf{k}_n^l = R_n W_K^l \mathbf{h}_n^l$, $\mathbf{v}_n^l = W_V^l \mathbf{h}_n^l$, where $\mathbf{q}_n^l, \mathbf{k}_n^l, \mathbf{v}_n^l \in \mathbb{R}^d$ denotes the Q, K, V values for the n -th input token, W_Q^l, W_K^l, W_V^l refer to the corresponding projection weight matrices, and R_n is the position embedding at position n , such as rotary position embedding (RoPE) [37]. During autoregressive decoding, the model repeatedly attends to all past positions, and stores every $(\mathbf{k}_n^l, \mathbf{v}_n^l)$ pair in GPU memory, known as *KV-cache*. Therefore, prefetching a prompt of N tokens costs $\mathcal{O}(N^2 d)$ multiply-adds per layer, dominating inference latency for long contexts. Since RoPE applies the fixed rotation matrix to both Key and Query at each position, cached

keys remain valid across subsequent steps with no further arithmetic modification, making KV-cache reuse the primary source of speed-ups in subsequent prefilling and decoding.

Directed-Graph Multi-agent Systems. Following [57, 69, 65], we model a multi-agent system as a directed graph $\mathcal{G} = (\mathcal{M}, \mathcal{E})$ whose nodes $m \in \mathcal{M}$ are *agents* and edges $e = (m_s \rightarrow m_t) \in \mathcal{E}$ denote one-way message passing from the m_s -th agent to the m_t -th agent. At interaction step t , the m -th agent composes an input prompt $\mathbf{s}_m^{(t)}$ in the template consisting of (i) fixed *prefix segments* shared across all turns, and (ii) *placeholder segments* filled at runtime with user queries, tool results, or upstream agent outputs, as formulated as follows, where $\mathbf{p}_{(m,0)}$ is usually a role-specific system prompt, $\mathbf{p}_{(m,i)}$ is the subsequent prefix segment of the i -th placeholder $\phi_{(m,i)}^{(t)}$.

$$\mathbf{s}_m^{(t)} = [\mathbf{p}_{(m,0)}, \phi_{(m,1)}^{(t)}, \mathbf{p}_{(m,1)}, \phi_{(m,2)}^{(t)}, \mathbf{p}_{(m,2)}, \dots, \phi_{(m,i)}^{(t)}, \mathbf{p}_{(m,i)}]. \quad (1)$$

Our work targets a distinct yet practical setting: a *directed multi-agent graph* in which each node is an **identical RoPE-based LLM checkpoint** instantiated with a role-specific system template. Since agents differ in the length of both prefixes and incoming messages, none of the existing static policies can predict the correct positional and contextual shifts; misalignment either forces full recomputation or yields steep accuracy loss. We therefore develop a *training-free, prompt-adaptive* cache-sharing mechanism, termed KVCOMM, which estimates the true offset on the fly and maintains an online anchor pool to accommodate rapidly changing interaction patterns, reducing prefilling latency without sacrificing task performance. The overall workload of KVCOMM is illustrated in Figure 3, which proceeds as follows.

0. Initialization Before any user requests, all agents precompute and store the KV-caches for all prefix segments defined in their prompt templates.

1. Placeholder Readiness When a request arrives, each agent checks whether all placeholders' base KV-caches are available. Missing bases are precomputed in parallel. Newly generated placeholder KV-caches are then sent to the *anchor prediction module* to search the anchor pool for similar samples and enable reuse.

2. Reuse or Fallback Once all placeholder KV-caches are ready, the agent determines whether reusable KV-cache *deviations* exist for each placeholder. If none are found, standard dense pre-filling is used. For placeholders without reusable deviations, the agent computes the difference between their actual and base KV-caches and stores this deviation in the anchor pool to expand anchor coverage.

3. Offset Approximation If all placeholders have reusable deviations, the agent fetches the matched anchors, estimates the KV-cache deviations via Eq. (6) and Eq. (7), and updates the placeholder and prefix KV-caches *in parallel*.

4. Decoding The agent concatenates the updated placeholder and prefix KV-caches and initiates response decoding.

5. Anchor Update After decoding, the produced KV-cache is passed through the anchor prediction module. If a similar anchor exists, the cache is stored in shared memory for future retrieval. The agent then waits for the next request.

6. Fallback Storage If no similar anchor exists, the response KV-cache is stored in the anchor pool so dependent agents can subsequently fill in deviations under their respective contexts; the agent then awaits the next request.

All inter-agent interactions occur through the *KV-cache Communication Module*. When multiple agents share the same user text but use different agent-specific prefixes, we avoid re-running prefilling by treating the KV-cache of the shared text under a new prefix as a *context-dependent offset* from its base KV-cache. We estimate this offset by interpolating from a small set of anchor examples, aligning Key positions via *RoPE de-rotation/re-rotation*, adding the estimated Key/Value offsets, then concatenating the adjusted segments and decoding.

Positional Alignment is Indispensable. Before analyzing two arbitrary tokens' cache correlation, we should first solve the position mismatch induced by RoPE. If a token is at position n in one prompt but at $n + \Delta$ in another, the raw keys differ by an orthogonal rotation R_Δ , whose difference can be orders of magnitude larger than the contextual deviation we care about, as demonstrated in Figure 1b. Hence, KVCOMM always de-rotates the stored key by $R_{-\Delta}$ before measuring similarity between

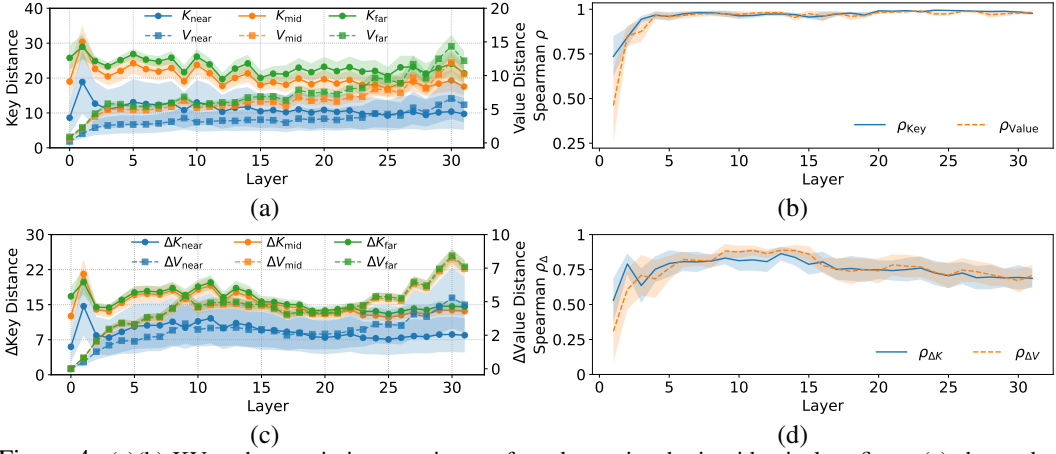


Figure 4: (a)(b) KV-cache proximity experiments for token pairs sharing identical prefixes: (a) shows the KV-cache distances (measured by ℓ_2 norm) across layers of the token pairs, which are grouped into “near”, “mid”, and “far” by embedding distance between the two tokens in the token pairs. (b) shows the Spearman [36] correlation between embedding distances and KV-cache proximity across layers. (c)(d) KV-cache offset proximity experiments for token pairs prefixed by two distinct contexts: (c) shows the layer-wise KV-cache offset distances between tokens grouped by embedding proximity. (d) shows the Spearman correlation between embedding distance and KV-cache offset proximity. Experimental details are shown in Appendix 6.3.1.

Key cache offsets of two tokens under the same context change. The following analysis assumes this alignment as completed so that the remaining deviations stem mainly from token identity and context.

3.2 Token-level Key/Value Similarity for KV Reuse

Motivation. KVCOMM hinges on the empirical observation that per-token KV vectors remain remarkably similar across distinct conversational contexts as long as the model parameters are shared. Intuitively, the residual pathway in every Transformer block keeps a copy of the input representation and adds the attention (Attn) and feed-forward (FFN) refinements:

$$\mathbf{h}_n^{l+1} = \mathbf{h}_n^l + \text{FFN}^l(\mathbf{h}_n^l + \text{Attn}^l(\mathbf{h}^l)_n), \quad (2)$$

where FFN^l and Attn^l refer to the FFN and Attn modules in the l -th layer. Hence, the identity information carried by the original embedding \mathbf{h}_n^l is never overwritten but *accumulates* across layers, suppressing the variation of the projected keys/values. Below we make this insight precise and quantify how far two distinct tokens are when prefixed with the same contexts.

Proposition 1 (KV-Distance Between Different Tokens). *Let \mathbf{k}_n^l and $\tilde{\mathbf{k}}_n^l$ be the key vectors of two different tokens at position n at layer l that are prefixed with the same token sequence. Assume Attn^l is α^l -Lipschitz, FFN^l is β^l -Lipschitz [20]. Define $\sigma^l \triangleq \beta^l(1 + n\alpha^l)$. Then*

$$\|\mathbf{k}_n^l - \tilde{\mathbf{k}}_n^l\| \leq C_R C_K^l \prod_{j=1}^{l-1} (1 + \sigma^j) \delta_n, \quad \delta_n = \max_{k \leq n} \|\mathbf{h}_k^1 - \tilde{\mathbf{h}}_k^1\|, \quad (3)$$

where $C_R > 0$ is related to RoPE and $C_K^l > 0$ is related to l -th layer projection key matrix W_K^l . Similarly, the inequality also holds for the value caches of the two tokens.

The proof is deferred to Appendix 6.2.2. It can be observed that Eq. (3) bounds the KV distance by the embedding gap scaled through layers, so tokens that start closer in embedding space have tighter bounds and greater cache-reuse potential. Figure 4a and 4b empirically demonstrate this insight, where the KV-caches of “near” token pairs are consistently closer to each other than the other two groups, and the KV-cache proximity is highly correlated to the token embedding distance.

We now examine this relation in multi-agent settings, where two similar tokens face different prefixes.

Proposition 2 (Deviation Proximity With Different Prefixes). *Let $\mathbf{k}_{n_a}^l$ and $\tilde{\mathbf{k}}_{n_a}^l$ be the key vectors of two different tokens at position n_a at layer l that are prefixed with prompt \mathbf{p}_a . Similarly, $\bar{\mathbf{k}}_{n_b}^l$ and $\tilde{\mathbf{k}}_{n_b}^l$ are the key vectors of the two tokens at position n_b at layer l that are prefixed with prompt \mathbf{p}_b . We denote the key cache deviation of each token at layer l by $\Delta^l = \bar{\mathbf{k}}_{n_b}^l - \mathbf{k}_{n_a}^l$, $\tilde{\Delta}^l = \tilde{\mathbf{k}}_{n_b}^l - \tilde{\mathbf{k}}_{n_a}^l$. Under the same Lipschitz assumptions as Proposition 1 and after positional alignment,*

$$\|\Delta^l - \tilde{\Delta}^l\| \leq 2C_R C_K^l \prod_{j=1}^{l-1} (1 + \sigma^j) \delta_{n_a}, \quad \delta_{n_a} = \max_{k \leq n_a} \|\mathbf{h}_k^1 - \tilde{\mathbf{h}}_k^1\|. \quad (4)$$

Similarly, the inequality also holds for the value caches of the two tokens.

Proof is in Appendix 6.2.2. Eq. (4) shows that tighter embedding gaps again yield smaller deviation bounds, supporting cross-context offset reuse. Figs. 4c and 4d validate this under the same setup as Figure 4a, with each token evaluated under two distinct prefixes, where the KV-cache offsets of “near” token pairs are also consistently closer to each other than the other two groups, and the KV-cache offset proximity is also highly correlated to the token embedding distance.

The above propositions motivate an anchor-based KV-sharing scheme that stores representative offsets as reusable anchors for future agent interactions to reduce all redundant prefilling latency of agents.

3.3 Anchor-based KV-cache Communication

We now introduce our anchor-based communication framework to unify the KV-cache sharing mechanism in multi-agent systems. During setup, each agent extracts placeholder information from its role-specific prompt into a structured dictionary, indicating token positions. The naming conventions for placeholders are detailed in Appendix 6.2.3. Each placeholder initializes an individual anchor pool upon receiving the first sample.

At runtime, subsequent input samples trigger a reuse check across agent placeholders. Agents reuse KV-caches directly from corresponding anchor pools if reuse conditions are satisfied, significantly speeding up inference by skipping redundant prefilling. Otherwise, agents revert to standard prefilling, updating anchor pools with newly computed KV-caches to enrich future reuse opportunities.

Anchor Pool Design. An anchor pool stores key information for each placeholder sample: (1) the base KV-cache, computed independently without external contexts; (2) offsets between the base and actual KV-caches within each agent’s context; and (3) offsets of subsequent neighboring prefix segment’s KV-cache. Thus, an anchor is represented as {ph_name: base KV, agent_id_ph: placeholder_offset, agent_id_pf: prefix_offset}. Neighboring prefix offsets are crucial due to position-dependent KV-cache shifts introduced by the placeholder’s context changes, as highlighted by the sink attention mechanism [53], which emphasizes local contextual dependencies.

Anchor Prediction. Determining whether newly-generated KV-caches, *e.g.*, responses, user inputs, etc., could be shared or treated as new anchors involves evaluating the embedding-based proximity [61, 29, 64, 59] and token length compatibility with existing anchors. The prediction criterion is designed as follows:

$$\mathcal{P}_{\text{anchor}}(\phi) = (\mathcal{L}_\phi > \max_{\psi \in \mathcal{A}} \mathcal{L}_\psi) \cup (\mathcal{H}_{\phi|\mathcal{A}} > \gamma \log |\mathcal{A}_\phi|), \quad \mathcal{H}_{\phi|\mathcal{A}} = \sum_{\psi \in \mathcal{A}_\phi} w_{\phi \rightarrow \psi} \log w_{\phi \rightarrow \psi}, \quad (5)$$

where \mathcal{A} refers to the anchor pool that the placeholder ϕ belongs to, ψ denotes an anchor in \mathcal{A} , \mathcal{L}_* represents the sequence length of the sample \star , $\mathcal{H}_{\phi|\mathcal{A}}$ measures entropy of the embedding-distance-based weights among longer anchors in the anchor pool, $w_{\phi \rightarrow \psi} = \text{softmax}(-\|\mathbf{h}_\phi - \mathbf{h}_\psi\|)$, $\psi \in \mathcal{A}_\phi$, $|\mathcal{A}_\phi|$ refers to the number of anchors longer than ϕ in $|\mathcal{A}|$, and γ is a threshold to determine how far a shareable sample could be away from the anchors of \mathcal{A} in the embedding space. Intuitively, anchors closer in embedding space yield more reliable offset predictions (validated by Prop. 2 and Figure 4c), and length compatibility ensures correct positional alignment (see Figure 1b).

Anchor Update. When KV-cache sharing criteria are unmet, the newly-generated cache becomes a new anchor’s base KV-cache. Agents relying on this unshareable placeholder revert to regular prefilling, providing agent-specific offsets for both the placeholder and its neighboring prefix segments to populate the new anchor entry. Due to GPU memory constraints, we implement an adaptive anchor pruning strategy: once anchor pools reach a predefined size \mathcal{V} , the least frequently accessed anchor among the earliest-added entries is discarded, maintaining a relevant and efficient anchor repository.

3.4 Anchor-based Cache Update

When placeholders in an agent’s prompt are predicted shareable, we efficiently update their KV-caches via anchor matching and offset approximation.

Anchor Matching. We retrieve reliable anchors identified during prediction, performing parallel reads due to independent addressing, leading to negligible overhead compared to traditional prefilling.

Offset Approximation. Using matched anchors, we approximate placeholders’ KV-caches within agent-specific contexts. Neighboring prefix segments are updated similarly based on the placeholder

Table 1: Performance of three cache-management strategies under different numbers of collaborating agents. Accuracy is reported for MMLU and GSM8K (Llama-3.1-8B-Instruct); Pass@1 is reported for HumanEval (Qwen-2.5-coder-7B). Higher is better. In addition, the Reuse Rate is reported for both KVCOMM and CacheBlend. Note that the Reuse Rate for CacheBlend is defined as the proportion of tokens reusing KV-caches in whole token sequences, while the Reuse Rate of KVCOMM is defined as *the frequency of agents reusing all KV-caches in the whole serving procedure*.

Dataset	Metric	Method	# Agents			
			2	3	4	5
MMLU	Accuracy (%)	Original	47.1	66.7	68.0	69.9
		CacheBlend	65.4	65.4	65.4	67.3
	Reuse Rate (%)	KVCOMM	64.7	68.6	68.0	69.9
		Original	0	0	0	0
	Reuse Rate (%)	CacheBlend	80	80	80	80
		KVCOMM	74.5	69.9	70.1	67.6
GSM8K	Accuracy (%)	Original	81.1	82.4	82.1	81.7
		CacheBlend	82.0	75.1	65.1	57.1
	Reuse Rate (%)	KVCOMM	81.5	81.7	80.6	79.6
		Original	0	0	0	0
	Reuse Rate (%)	CacheBlend	80	80	80	80
		KVCOMM	79.6	77.0	73.4	71.0
HumanEval	Pass@1 (%)	Original	86.3	83.9	84.5	85.1
		CacheBlend	31.1	21.1	30.4	32.9
	Reuse Rate (%)	KVCOMM	81.4	83.2	83.2	83.2
		Original	0	0	0	0
	Reuse Rate (%)	CacheBlend	80	80	80	80
		KVCOMM	87.6	84.7	81.1	77.8

sample's embedding proximity. Formally, the KV-cache of the i -th placeholder in the m -th agent is approximated as follows:

$$(\hat{\mathbf{k}}/\hat{\mathbf{v}})_{\phi(m,i)} = (\mathbf{k}/\mathbf{v})_{\phi(m,i)} + \sum_{\psi \in \mathcal{A}_{\phi(m,i)}} w_{\phi(m,i) \rightarrow \psi} \cdot \Delta(\mathbf{k}/\mathbf{v})_{(m,\psi)}^{\phi}, \quad (6)$$

where $(\hat{\mathbf{k}}/\hat{\mathbf{v}})_{\phi(m,i)}$ refers to the approximated KV cache for the placeholder $\phi(m,i)$. $(\mathbf{k}/\mathbf{v})_{\phi(m,i)}$ is the base KV cache for the placeholder $\phi(m,i)$. $w_{\phi(m,i) \rightarrow \psi}$ is the softmax mapping of $-\|\mathbf{h}_{\phi(m,i)} - \mathbf{h}_{\psi}\|$ across the anchor dimension. $\Delta(\mathbf{k}/\mathbf{v})_{(m,\psi)}^{\phi}$ is the placeholder ϕ 's cache offsets in the m -th agent for the anchor ψ . Prefix segment updates follow an analogous process:

$$(\hat{\mathbf{k}}/\hat{\mathbf{v}})_{\mathbf{p}(m,i)} = (\mathbf{k}/\mathbf{v})_{\mathbf{p}(m,i)} + \sum_{\psi \in \mathcal{A}_{\phi(m,i)}} w_{\phi(m,i) \rightarrow \psi} \cdot \Delta(\mathbf{k}/\mathbf{v})_{(m,\psi)}^{\mathbf{p}}, \quad (7)$$

where $(\hat{\mathbf{k}}/\hat{\mathbf{v}})_{\mathbf{p}(m,i)}$ refers to the approximated KV cache for the prefix segment $\mathbf{p}(m,i)$. $(\mathbf{k}/\mathbf{v})_{\mathbf{p}(m,i)}$ is the base KV cache for the prefix segment $\mathbf{p}(m,i)$. $\Delta(\mathbf{k}/\mathbf{v})_{(m,\psi)}^{\mathbf{p}}$ is the corresponding prefix segment's cache offset in the m -th agent for the anchor ψ .

After approximation, updated caches are concatenated and directly fed into decoding, substantially reducing prefilling latency via parallel processing. The overall algorithm is listed in Appendix 6.2.5.

4 Experiments

4.1 Experimental Setup

Multi-agent System. Following GPTSwarm [69] and AgentPrune [65], we construct a fully-connected multi-agent system with established techniques including few-shot prompting [2], chain-of-thought [45], function calling [33], and structured outputs [34]. To precisely analyze KV-cache behaviors, we deploy open-source models using HuggingFace's framework rather than closed-source APIs used by AgentPrune. Specifically, we employ Llama-3.1-8B-Instruct [11] (Llama-3.1) for retrieval-augmented generation (RAG) and math reasoning, and Qwen-Coder-2.5-7B-Instruct [16] for programming tasks. We evaluate performance across scenarios ranging from two to five agents.

Benchmark Datasets. We assess RAG performance using MMLU [13], math reasoning with GSM8K [7], and programming capability via HumanEval [4].

Table 2: Per-agent TTFT breakdown and speedup. Table 3: Mean TTFT speedup using Llama-3.1.
(Prefix token length per agent: 512; Output token length: 512; Model: Llama-3.1; #Agents = 5)

TTFT (ms)	Agent 1	Agent 2	Agent 3	Agent 4	Agent 5
Original	125.8	192.4	258.3	330.9	428.6
KVCOMM	5.5	7.7	10.2	13.5	17.5
1 st Token Decode	21.4	21.2	21.2	21.3	21.1
Others	86.6	9.1	10.7	13.5	16.2
Speedup	1.11x	5.06x	6.14x	6.85x	7.82x

Out_len	In_len (Prefix sequence)				
	64	128	256	512	1024
128	2.24x	2.31x	2.56x	3.07x	4.45x
256	2.50x	2.51x	2.83x	3.44x	4.75x
512	3.05x	3.18x	3.49x	4.09x	5.34x
1024	4.40x	4.48x	4.75x	5.35x	6.72x

Comparison Baselines. To our knowledge, KVCOMM is the first method enabling comprehensive KV-cache sharing tailored for open-source multi-agent frameworks. Hence, we compare primarily against CacheBlend [58], which selectively recomputes sensitive tokens’ caches for partial reuse. Given CacheBlend’s tight integration with vLLM [21], we faithfully replicate its selective recomputation strategy within our experimental setup, consistently recomputing the top-20% tokens exhibiting the largest KV deviations, ensuring fair baseline alignment.

Evaluation Metrics. We report Accuracy scores on MMLU and GSM8K, and Pass@1 for coding tasks. Efficiency metrics include Reuse Rate (meaning the proportion of agents employing the cache reuse scheme), individual agent Time-To-First-Token (TTFT), and average TTFT across agents.

Implementation Details. Experiments are executed on a single NVIDIA H100 GPU. The maximum generation length is uniformly set to 512 tokens, with hyperparameters selected as $\gamma = 0.3$ and anchor pool size $\mathcal{V} = 20$. Further implementation specifics are detailed in Appendix 6.3.

4.2 Main Results

Table 1 compares our KVCOMM approach with the Original (no cache reuse) and CacheBlend [58] strategies across multiple agent configurations. Although our agent prompts were initially optimized for closed-source models, causing some performance drops with open-source deployments, KVCOMM still maintains or improves upon baseline accuracy.

On MMLU, KVCOMM achieves competitive accuracy (64.7%–69.9%), consistently outperforming or matching CacheBlend and closely tracking the original baseline. This indicates robust cross-context KV-cache alignment by KVCOMM. CacheBlend fluctuates significantly with increasing agents. The reason why the baseline method performs poorly on the MMLU benchmark under the two-agent setting is that the first agent is designed as the *knowledgeable expert* to produce the related key words about the user question, and the second agent is designed as the *Final Refer* to analyze the predecessor agents’ output and give the answer based on the previous agent’s output, where the failure cases mainly occur when the second agent only output the answer without analysis. The prompt of each agent can be found in Appendix 6.3.2.

For GSM8K math reasoning, KVCOMM’s accuracy remains stable, only declining by 1.9% (81.5%→79.6%) from two to five agents, maintaining within $\pm 2\%$ of the original baseline. In contrast, CacheBlend’s accuracy drops dramatically from 82.0% to 57.1%, highlighting the necessity for precise KV-cache reuse in numerical tasks.

In the HumanEval coding benchmark, KVCOMM delivers stable Pass@1 scores (81.4%–83.2%), significantly surpassing CacheBlend by an average margin of 53%. This underscores KVCOMM’s ability to preserve task-critical dependencies essential for programming tasks. The severe performance degradation of CacheBlend on Humaneval attributes to the diverse syntax separators involved in the generation process (e.g., ., ;, !), which induce diverse and prefix-sensitive KV-cache distributions.

Reuse Rate. Unlike CacheBlend’s fixed reuse strategy (80%), KVCOMM adaptively determines KV-cache reuse, consistently achieving high reuse rates (70%–87.6%). This rate naturally declines as agent number increases due to more diverse contexts, but KVCOMM still effectively identifies shareable caches, confirming that adaptive reuse avoids context degradation.

4.3 Results of TTFT Speedup¹

Table 2 reports TTFT per agent receiving 1K tokens from user input with 512 prefix tokens and sharing the 512 response tokens with succeeding agents. The first agent, lacking upstream caches

¹In the original submission, the TTFT calculation for KVCOMM omitted the first token’s decoding latency. The final version rectifies this.

(costing 86.6ms in “other” operations), shows modest acceleration ($1.11\times$). Subsequent agents reduce prefilling dramatically to 26.9–38.6 ms via KVCOMM, achieving up to $7.82\times$ speedup (Agent 5).

Scalability in Context Length. We further examine scalability in Table 3, varying prefix (64–1K tokens) and output lengths (128–1K tokens) among three collaborating agents. KVCOMM achieves a minimum mean speedup of $2.24\times$ (shortest setting) and scales effectively to $6.72\times$ (longest setting), validating the approach’s efficiency gain as context length and complexity increase.

4.4 Discussion and Ablation Study

Robustness to Request Order. Table 4 examines how request ordering affects KVCOMM’s cache alignment using MMLU. We test two random orders (Rand-1, Rand-2), ascending and descending length orders. It can be observed that performance is correlated with request order due to the designed anchor prediction criterion. Results confirm KVCOMM is robust across diverse ordering strategies, achieving consistent or slightly improved accuracy compared to the baseline, demonstrating minimal sensitivity to request sequence variability.

Contribution of Each Alignment Step. Table 5 details ablation results for three alignment components on MMLU under a four-agent setting: (1) position alignment via key rotation, (2) placeholder KV-cache offset, and (3) prefix segment KV-cache offset. The results reveal that each alignment step is critical; omitting any severely degrades accuracy. Although combining key rotation and prefix offset achieves 62.1% accuracy, the response of each agent is visibly less coherent with the original one (See Appendix 6.4.6). Therefore, complete alignment is essential for robust cross-context performance.

Sensitivity to Hyperparameters. Table 6 explores KVCOMM’s sensitivity to the entropy threshold γ and anchor pool size \mathcal{V} using GSM8K with four agents. $\gamma = 0 / \mathcal{V} = 0$ refers to the original no-cache-sharing method. It can be observed that with conservative reuse ($\gamma = 0.1$), accuracy improves slightly (1%), while moderate relaxation significantly boosts reuse (up to 98.2%) at minimal accuracy cost (3.3%). For \mathcal{V} , performance is relatively stable with the increase of stored anchors, while the reuse rate finally becomes stable at 73.4%, indicating that $\mathcal{V} = 20$ effectively balances efficiency and task performance.

5 Conclusion

In this paper, we explore KV-cache sharing for efficient communication in collaborative LLM-based MAS and introduce KVCOMM, a drop-in framework to enable efficient agent communication through shared KV-cache reuse and context-aware cache offsetting. Besides, we perform analyses of KV-cache deviation across varying prefix contexts, and propose an anchor-based offset estimator to effectively align and reuse shared context KV-caches. Extensive experiments conducted on Retrieval-Augmented Generation (RAG), Math Reasoning, and Programming-related multi-agent systems demonstrate that our method provides an effective trade-off between prefilling efficiency and system accuracy, continuously reducing average latency as the number of agents increases. Specifically, KVCOMM can achieve $\sim 6.7\times$ average prefilling speedup under the three-agent setting on a single H100 GPU, significantly improving the deployment efficiency of collaborative multi-agent language models.

Table 4: Study on the robustness to varying request orders. Accuracy is reported. (#Agent = 4, Baseline Acc = 68.0%; Model: Llama3.1)

Method	Rand-1	Rand-2	Ascending	Descending
KVCOMM	68.0	72.5	67.3	66.0

k w/ rot	ϕ w/ offset	p w/ offset	Acc (%)
✓			43.1%
	✓		58.8%
		✓	60.1%
✓	✓		38.6%
✓		✓	62.1%
	✓	✓	56.9%
✓	✓	✓	68.0%

Table 5: Ablation study on MMLU under four-agent setting. (Model: Llama-3.1)

Metric	Threshold γ ($\mathcal{V} = 20$)					
	0	0.1	0.3	0.5	0.7	0.9
Accuracy (%)	82.1	83.1	80.6	80.0	78.9	78.8
Reuse rate (%)	N/A	34.3	73.4	94.9	97.5	98.2
Maximum Anchor Num \mathcal{V} ($\gamma = 0.3$)						
Metric	0	5	10	15	20	25
Accuracy (%)	82.1	82.0	81.4	81.2	80.6	80.6
Reuse rate (%)	N/A	44.0	60.3	66.2	73.4	73.4

Table 6: Hyperparameter analysis on GSM8K under the four-agent setting using Llama-3.1.

Acknowledgments

Hancheng Ye, Jianyi Zhang, and Yiran Chen disclose the support from NSF 2112562, ARO W911NF-23-2-0224, and NAIRR Pilot project NAIRR240270. Danyang Zhuo discloses the support from NSF 2503010. We sincerely thank the program chairs, area chair, and reviewers for their valuable comments.

References

- [1] Josh Achiam, Steven Adler, Sandhini Agarwal, Lama Ahmad, Ilge Akkaya, Florencia Leoni Aleman, Diogo Almeida, Janko Altenschmidt, Sam Altman, Shyamal Anadkat, et al. Gpt-4 technical report. *arXiv preprint arXiv:2303.08774*, 2023.
- [2] Tom Brown, Benjamin Mann, Nick Ryder, Melanie Subbiah, Jared D Kaplan, Prafulla Dhariwal, Arvind Neelakantan, Pranav Shyam, Girish Sastry, Amanda Askell, et al. Language models are few-shot learners. *Advances in neural information processing systems*, 33:1877–1901, 2020.
- [3] Chen-Chia Chang, Chia-Tung Ho, Yuguang Li, Yiran Chen, and Haoxing Ren. Drc-coder: Automated drc checker code generation using llm autonomous agent. In *Proceedings of the 2025 International Symposium on Physical Design*, pages 143–151, 2025.
- [4] Mark Chen, Jerry Tworek, Heewoo Jun, Qiming Yuan, Henrique Ponde de Oliveira Pinto, Jared Kaplan, Harri Edwards, Yuri Burda, Nicholas Joseph, Greg Brockman, Alex Ray, Raul Puri, Gretchen Krueger, Michael Petrov, Heidy Khlaaf, Girish Sastry, Pamela Mishkin, Brooke Chan, Scott Gray, Nick Ryder, Mikhail Pavlov, Alethea Power, Lukasz Kaiser, Mohammad Bavarian, Clemens Winter, Philippe Tillett, Felipe Petroski Such, Dave Cummings, Matthias Plappert, Fotios Chantzis, Elizabeth Barnes, Ariel Herbert-Voss, William Hebbgen Guss, Alex Nichol, Alex Paino, Nikolas Tezak, Jie Tang, Igor Babuschkin, Suchir Balaji, Shantanu Jain, William Saunders, Christopher Hesse, Andrew N. Carr, Jan Leike, Josh Achiam, Vedant Misra, Evan Morikawa, Alec Radford, Matthew Knight, Miles Brundage, Mira Murati, Katie Mayer, Peter Welinder, Bob McGrew, Dario Amodei, Sam McCandlish, Ilya Sutskever, and Wojciech Zaremba. Evaluating large language models trained on code. 2021.
- [5] Yihua Cheng, Yuhan Liu, Jiayi Yao, Yuwei An, Xiaokun Chen, Shaoting Feng, Yuyang Huang, Samuel Shen, Kuntai Du, and Junchen Jiang. Lmcache: An efficient kv cache layer for enterprise-scale llm inference. *arXiv preprint arXiv:2510.09665*, 2025.
- [6] ChuGyouk. Aime-22-25. Hugging Face Dataset, 2025. <https://huggingface.co/datasets/ChuGyouk/AIME-22-25>.
- [7] Karl Cobbe, Vineet Kosaraju, Mohammad Bavarian, Mark Chen, Heewoo Jun, Lukasz Kaiser, Matthias Plappert, Jerry Tworek, Jacob Hilton, Reiichiro Nakano, Christopher Hesse, and John Schulman. Training verifiers to solve math word problems. *arXiv preprint arXiv:2110.14168*, 2021.
- [8] Yuzhe Fu, Changchun Zhou, Tianling Huang, Eryi Han, Yifan He, and Hailong Jiao. Softact: A high-precision softmax architecture for transformers supporting nonlinear functions. *IEEE Transactions on Circuits and Systems for Video Technology*, 34(9):8912–8923, 2024.
- [9] Yingqiang Ge, Wenyue Hua, Kai Mei, Jianchao Ji, Juntao Tan, Shuyuan Xu, Zelong Li, and Yongfeng Zhang. Openagi: When llm meets domain experts. In *Advances in Neural Information Processing Systems (NeurIPS)*, 2023.
- [10] In Gim, Guojun Chen, Seung-seob Lee, Nikhil Sarda, Anurag Khandelwal, and Lin Zhong. Prompt cache: Modular attention reuse for low-latency inference. *Proceedings of Machine Learning and Systems*, 6:325–338, 2024.
- [11] Aaron Grattafiori, Abhimanyu Dubey, Abhinav Jauhri, Abhinav Pandey, Abhishek Kadian, Ahmad Al-Dahle, Aiesha Letman, Akhil Mathur, Alan Schelten, Alex Vaughan, et al. The llama 3 herd of models. *arXiv preprint arXiv:2407.21783*, 2024.
- [12] Daya Guo, Dejian Yang, Haowei Zhang, Junxiao Song, Ruoyu Zhang, Runxin Xu, Qihao Zhu, Shirong Ma, Peiyi Wang, Xiao Bi, et al. Deepseek-r1: Incentivizing reasoning capability in llms via reinforcement learning. *arXiv preprint arXiv:2501.12948*, 2025.
- [13] Dan Hendrycks, Collin Burns, Steven Basart, Andy Zou, Mantas Mazeika, Dawn Song, and Jacob Steinhardt. Measuring massive multitask language understanding. In *International Conference on Learning Representations*.

- [14] Dan Hendrycks, Collin Burns, Saurav Kadavath, Akul Arora, Steven Basart, Eric Tang, Dawn Song, and Jacob Steinhardt. Measuring mathematical problem solving with the math dataset. In *Thirty-fifth Conference on Neural Information Processing Systems Datasets and Benchmarks Track (Round 2)*.
- [15] Matthew Ho, Chen Si, Zhaoxiang Feng, Fangxu Yu, Zhijian Liu, Zhiteng Hu, and Lianhui Qin. Arcmemo: Abstract reasoning composition with lifelong llm memory. *arXiv preprint arXiv:2509.04439*, 2025.
- [16] Binyuan Hui, Jian Yang, Zeyu Cui, Jiaxi Yang, Dayiheng Liu, Lei Zhang, Tianyu Liu, Jiajun Zhang, Bowen Yu, Kai Dang, et al. Qwen2. 5-coder technical report. *arXiv preprint arXiv:2409.12186*, 2024.
- [17] Chao Huang Jiabin Tang, Tianyu Fan. AutoAgent: A Fully-Automated and Zero-Code Framework for LLM Agents, 2025.
- [18] Ting Jiang, Yixiao Wang, Hancheng Ye, Zishan Shao, Jingwei Sun, Jingyang Zhang, Zekai Chen, Jianyi Zhang, Yiran Chen, and Hai Li. Sada: Stability-guided adaptive diffusion acceleration. *arXiv preprint arXiv:2507.17135*, 2025.
- [19] YICHEN JIANG, SUORONG YANG, SHENGJI TANG, SHENGHE ZHENG, and JIANJIAN CAO. A comprehensive survey of llm-driven collective intelligence: Past, present, and future. 2025.
- [20] Hyunjik Kim, George Papamakarios, and Andriy Mnih. The lipschitz constant of self-attention. In *International Conference on Machine Learning*, pages 5562–5571. PMLR, 2021.
- [21] Woosuk Kwon, Zhuohan Li, Siyuan Zhuang, Ying Sheng, Lianmin Zheng, Cody Hao Yu, Joseph E. Gonzalez, Hao Zhang, and Ion Stoica. Efficient memory management for large language model serving with pagedattention. In *Proceedings of the ACM SIGOPS 29th Symposium on Operating Systems Principles*, 2023.
- [22] Guohao Li, Hasan Abed Al Kader Hammoud, Hani Itani, Dmitrii Khizbulin, and Bernard Ghanem. Camel: Communicative agents for "mind" exploration of large language model society. In *Thirty-seventh Conference on Neural Information Processing Systems*, 2023.
- [23] Yueqian Lin, Yuzhe Fu, Jingyang Zhang, Yudong Liu, Jianyi Zhang, Jingwei Sun, Hai Li, Yiran Chen, et al. Speechprune: Context-aware token pruning for speech information retrieval. *arXiv preprint arXiv:2412.12009*, 2024.
- [24] Yueqian Lin, Qinsi Wang, Hancheng Ye, Yuzhe Fu, Hai Li, Yiran Chen, et al. Hippomm: Hippocampal-inspired multimodal memory for long audiovisual event understanding. *arXiv preprint arXiv:2504.10739*, 2025.
- [25] Aixin Liu, Bei Feng, Bin Wang, Bingxuan Wang, Bo Liu, Chenggang Zhao, Chengqi Dengr, Chong Ruan, Damai Dai, Daya Guo, et al. Deepseek-v2: A strong, economical, and efficient mixture-of-experts language model. *arXiv preprint arXiv:2405.04434*, 2024.
- [26] Jijia Liu, Chao Yu, Jiaxuan Gao, Yuqing Xie, Qingmin Liao, Yi Wu, and Yu Wang. Llm-powered hierarchical language agent for real-time human-ai coordination. *arXiv preprint arXiv:2312.15224*, 2023.
- [27] Yuhan Liu, Yuyang Huang, Jiayi Yao, Zhuohan Gu, Kuntai Du, Hanchen Li, Yihua Cheng, Junchen Jiang, Shan Lu, Madan Musuvathi, et al. Droidspeak: Kv cache sharing for cross-llm communication and multi-llm serving. *arXiv preprint arXiv:2411.02820*, 2024.
- [28] Yuhan Liu, Hanchen Li, Yihua Cheng, Siddhant Ray, Yuyang Huang, Qizheng Zhang, Kuntai Du, Jiayi Yao, Shan Lu, Ganesh Ananthanarayanan, et al. Cachegen: Kv cache compression and streaming for fast large language model serving. In *Proceedings of the ACM SIGCOMM 2024 Conference*, pages 38–56, 2024.
- [29] Diego Mesquita, Amauri Souza, and Samuel Kaski. Rethinking pooling in graph neural networks. *Advances in Neural Information Processing Systems*, 33:2220–2231, 2020.
- [30] Mozhgan Navardi, Romina Aalishah, Yuzhe Fu, Yueqian Lin, Hai Li, Yiran Chen, and Tinoosh Mohsenin. Genai at the edge: Comprehensive survey on empowering edge devices. In *Proceedings of the AAAI Symposium Series*, volume 5, pages 180–187, 2025.
- [31] Joon Sung Park, Joseph O’Brien, Carrie Jun Cai, Meredith Ringel Morris, Percy Liang, and Michael S Bernstein. Generative agents: Interactive simulacra of human behavior. In *Proceedings of the 36th annual acm symposium on user interface software and technology*, pages 1–22, 2023.
- [32] Bharat Prakash, Tim Oates, and Tinoosh Mohsenin. Llm augmented hierarchical agents. In *NeurIPS 2023 Foundation Models for Decision Making Workshop*.

- [33] Yujia Qin, Shihao Liang, Yining Ye, Kunlun Zhu, Lan Yan, Yaxi Lu, Yankai Lin, Xin Cong, Xiangru Tang, Bill Qian, et al. Toolllm: Facilitating large language models to master 16000+ real-world apis. *arXiv preprint arXiv:2307.16789*, 2023.
- [34] Connor Shorten, Charles Pierse, Thomas Benjamin Smith, Erika Cardenas, Akanksha Sharma, John Trengrove, and Bob van Luijt. Structuredrag: Json response formatting with large language models. *arXiv preprint arXiv:2408.11061*, 2024.
- [35] Significant Gravitas. AutoGPT.
- [36] Charles Spearman. The proof and measurement of association between two things. *The American journal of psychology*, 100(3/4):441–471, 1987.
- [37] Jianlin Su, Murtadha Ahmed, Yu Lu, Shengfeng Pan, Wen Bo, and Yunfeng Liu. Roformer: Enhanced transformer with rotary position embedding. *Neurocomputing*, 568:127063, 2024.
- [38] Khanh-Tung Tran, Dung Dao, Minh-Duong Nguyen, Quoc-Viet Pham, Barry O’Sullivan, and Hoang D Nguyen. Multi-agent collaboration mechanisms: A survey of llms. *arXiv preprint arXiv:2501.06322*, 2025.
- [39] Guanzhi Wang, Yuqi Xie, Yunfan Jiang, Ajay Mandlekar, Chaowei Xiao, Yuke Zhu, Linxi Fan, and Anima Anandkumar. Voyager: An open-ended embodied agent with large language models. *Transactions on Machine Learning Research*.
- [40] Qinsi Wang, Jinghan Ke, Masayoshi Tomizuka, Yiran Chen, Kurt Keutzer, and Chenfeng Xu. Dobi-svd: Differentiable svd for llm compression and some new perspectives. *arXiv preprint arXiv:2502.02723*, 2025.
- [41] Qinsi Wang, Jinghan Ke, Hancheng Ye, Yueqian Lin, Yuzhe Fu, Jianyi Zhang, Kurt Keutzer, Chenfeng Xu, and Yiran Chen. Angles don’t lie: Unlocking training-efficient rl through the model’s own signals. *arXiv preprint arXiv:2506.02281*, 2025.
- [42] Qinsi Wang, Bo Liu, Tianyi Zhou, Jing Shi, Yueqian Lin, Yiran Chen, Hai Helen Li, Kun Wan, and Wentian Zhao. Vision-zero: Scalable vlm self-improvement via strategic gamified self-play, 2025.
- [43] Qinsi Wang, Saeed Vahidian, Hancheng Ye, Jianyang Gu, Jianyi Zhang, and Yiran Chen. Coreinfer: Accelerating large language model inference with semantics-inspired adaptive sparse activation. *arXiv preprint arXiv:2410.18311*, 2024.
- [44] Qinsi Wang, Hancheng Ye, Ming-Yu Chung, Yudong Liu, Yueqian Lin, Martin Kuo, Mingyuan Ma, Jianyi Zhang, and Yiran Chen. Corematching: A co-adaptive sparse inference framework with token and neuron pruning for comprehensive acceleration of vision-language models. *arXiv preprint arXiv:2505.19235*, 2025.
- [45] Jason Wei, Xuezhi Wang, Dale Schuurmans, Maarten Bosma, Fei Xia, Ed Chi, Quoc V Le, Denny Zhou, et al. Chain-of-thought prompting elicits reasoning in large language models. *Advances in neural information processing systems*, 35:24824–24837, 2022.
- [46] Bingyang Wu, Shengyu Liu, Yinmin Zhong, Peng Sun, Xuanzhe Liu, and Xin Jin. Loongserve: Efficiently serving long-context large language models with elastic sequence parallelism. In *Proceedings of the ACM SIGOPS 30th Symposium on Operating Systems Principles*, pages 640–654, 2024.
- [47] Chengyue Wu, Hao Zhang, Shuchen Xue, Zhijian Liu, Shizhe Diao, Ligeng Zhu, Ping Luo, Song Han, and Enze Xie. Fast-dllm: Training-free acceleration of diffusion llm by enabling kv cache and parallel decoding. *arXiv preprint arXiv:2505.22618*, 2025.
- [48] Qingyun Wu, Gagan Bansal, Jieyu Zhang, Yiran Wu, Beibin Li, Erkang Zhu, Li Jiang, Xiaoyun Zhang, Shaokun Zhang, Jiale Liu, et al. Autogen: Enabling next-gen llm applications via multi-agent conversations. In *First Conference on Language Modeling*.
- [49] Yongji Wu, Yechen Xu, Jingrong Chen, Zhaodong Wang, Ying Zhang, Matthew Lentz, and Danyang Zhuo. Mccs: A service-based approach to collective communication for multi-tenant cloud. In *Proceedings of the ACM SIGCOMM 2024 Conference*, pages 679–690, 2024.
- [50] Chunqiu Steven Xia, Yinlin Deng, Soren Dunn, and Lingming Zhang. Agentless: Demystifying llm-based software engineering agents. *arXiv preprint arXiv:2407.01489*, 2024.
- [51] Renqiu Xia, Haoyang Peng, Hancheng Ye, Mingsheng Li, Xiangchao Yan, Peng Ye, Botian Shi, Yu Qiao, Junchi Yan, and Bo Zhang. Structchart: On the schema, metric, and augmentation for visual chart understanding. *arXiv e-prints*, pages arXiv–2309, 2023.

- [52] Renqiu Xia, Bo Zhang, Hancheng Ye, Xiangchao Yan, Qi Liu, Hongbin Zhou, Zijun Chen, Peng Ye, Min Dou, Botian Shi, et al. Chartx & chartvlm: A versatile benchmark and foundation model for complicated chart reasoning. *arXiv preprint arXiv:2402.12185*, 2024.
- [53] Guangxuan Xiao, Yuandong Tian, Beidi Chen, Song Han, and Mike Lewis. Efficient streaming language models with attention sinks. In *The Twelfth International Conference on Learning Representations*.
- [54] Yechen Xu, Xinhao Kong, Tingjun Chen, and Danyang Zhuo. Conveyor: Efficient tool-aware llm serving with tool partial execution. *arXiv preprint arXiv:2406.00059*, 2024.
- [55] Xiangchao Yan, Shiyang Feng, Jiakang Yuan, Renqiu Xia, Bin Wang, Bo Zhang, and Lei Bai. Surveyforge: On the outline heuristics, memory-driven generation, and multi-dimensional evaluation for automated survey writing. *arXiv preprint arXiv:2503.04629*, 2025.
- [56] Jingbo Yang, Bairu Hou, Wei Wei, Yujia Bao, and Shiyu Chang. Kvlink: Accelerating large language models via efficient kv cache reuse. *arXiv preprint arXiv:2502.16002*, 2025.
- [57] Yuhao Yang, Jiaxin Tang, Lianghao Xia, Xingchen Zou, Yuxuan Liang, and Chao Huang. Graphagent: Agentic graph language assistant. *arXiv preprint arXiv:2412.17029*, 2024.
- [58] Jiayi Yao, Hanchen Li, Yuhua Liu, Siddhant Ray, Yihua Cheng, Qizheng Zhang, Kuntai Du, Shan Lu, and Junchen Jiang. Cacheblend: Fast large language model serving for rag with cached knowledge fusion. In *Proceedings of the Twentieth European Conference on Computer Systems*, pages 94–109, 2025.
- [59] Hancheng Ye, Chong Yu, Peng Ye, Renqiu Xia, Yansong Tang, Jiwen Lu, Tao Chen, and Bo Zhang. Once for both: Single stage of importance and sparsity search for vision transformer compression. In *Proceedings of the IEEE/CVF Conference on Computer Vision and Pattern Recognition*, pages 5578–5588, 2024.
- [60] Hancheng Ye, Jiakang Yuan, Renqiu Xia, Xiangchao Yan, Tao Chen, Junchi Yan, Botian Shi, and Bo Zhang. Training-free adaptive diffusion with bounded difference approximation strategy. *Advances in Neural Information Processing Systems*, 37:306–332, 2024.
- [61] Zhitao Ying, Jiaxuan You, Christopher Morris, Xiang Ren, Will Hamilton, and Jure Leskovec. Hierarchical graph representation learning with differentiable pooling. *Advances in neural information processing systems*, 31, 2018.
- [62] Jiakang Yuan, Xiangchao Yan, Botian Shi, Tao Chen, Wanli Ouyang, Bo Zhang, Lei Bai, Yu Qiao, and Bowen Zhou. Dolphin: Closed-loop open-ended auto-research through thinking, practice, and feedback. *arXiv preprint arXiv:2501.03916*, 2025.
- [63] Aohan Zeng, Mingdao Liu, Rui Lu, Bowen Wang, Xiao Liu, Yuxiao Dong, and Jie Tang. Agenttuning: Enabling generalized agent abilities for llms. In *Findings of the Association for Computational Linguistics ACL 2024*, pages 3053–3077, 2024.
- [64] Bo Zhang, Hancheng Ye, Gang Yu, Bin Wang, Yike Wu, Jiayuan Fan, and Tao Chen. Sample-centric feature generation for semi-supervised few-shot learning. *IEEE Transactions on Image Processing*, 31:2309–2320, 2022.
- [65] Guibin Zhang, Yanwei Yue, Zhixun Li, Sukwon Yun, Guancheng Wan, Kun Wang, Dawei Cheng, Jeffrey Xu Yu, and Tianlong Chen. Cut the crap: An economical communication pipeline for LLM-based multi-agent systems. In *The Thirteenth International Conference on Learning Representations*, 2025.
- [66] Lingzhe Zhang, Yunpeng Zhai, Tong Jia, Xiaosong Huang, Chiming Duan, and Ying Li. Agentfm: Role-aware failure management for distributed databases with llm-driven multi-agents. *arXiv preprint arXiv:2504.06614*, 2025.
- [67] Siyan Zhao, Daniel Israel, Guy Van den Broeck, and Aditya Grover. Prepacking: A simple method for fast prefilling and increased throughput in large language models. *arXiv preprint arXiv:2404.09529*, 2024.
- [68] Lianmin Zheng, Liangsheng Yin, Zhiqiang Xie, Chuyue Livia Sun, Jeff Huang, Cody Hao Yu, Shiyi Cao, Christos Kozyrakis, Ion Stoica, Joseph E Gonzalez, et al. Sqlang: Efficient execution of structured language model programs. *Advances in Neural Information Processing Systems*, 37:62557–62583, 2024.
- [69] Mingchen Zhuge, Wenyi Wang, Louis Kirsch, Francesco Faccio, Dmitrii Khizbulin, and Jürgen Schmidhuber. Gptswarm: Language agents as optimizable graphs. In *Forty-first International Conference on Machine Learning*, 2024.

6 Appendix

Due to the ten-page limitation of the manuscript, we provide more details and visualizations from the following aspects:

- Sec. 6.1: Limitations and Broader Impacts.
- Sec. 6.2: Method Explanation.
 - Sec. 6.2.1: Glossary.
 - Sec. 6.2.2: Theoretical Proof of Proposition 1 and 2.
 - Sec. 6.2.3: Placeholder Naming Rules.
 - Sec. 6.2.4: KV-cache Management System.
 - Sec. 6.2.5: Algorithm of KVCOMM.
- Sec. 6.3: More Experimental Details.
 - Sec. 6.3.1: Statistical Analysis of KV-cache Proximity and Offset Proximity.
 - Sec. 6.3.2: Prompts on Three Benchmarks.
- Sec. 6.4: More Experimental Analysis.
 - Sec. 6.4.1: Evaluations on Harder Reasoning Benchmarks
 - Sec. 6.4.2: Analysis on the Matching Criterion.
 - Sec. 6.4.3: Analysis on the Approximation Method.
 - Sec. 6.4.4: Analysis on the Overhead in Long-context Anchor Matching.
 - Sec. 6.4.5: Analysis on the Memory Cost of KVCOMM.
 - Sec. 6.4.6: Visualization of Responses Generated by Different Combinations of Alignment Strategies.
 - Sec. 6.4.7: Visualization of Anchor Distribution.
 - Sec. 6.4.8: Visualization of Difference between Prefix and Placeholder Offset Distributions.
 - Sec. 6.4.9: Visualization of Distance between Approximated and Real Offsets.

6.1 Limitations and Broader Impacts

Currently, KVCOMM is evaluated on LLM-based multi-agent systems that process text inputs. A long-term vision of multi-agent systems is to achieve lossless acceleration on any modality input, such as image, video, or audio input. Besides, although KVCOMM can accelerate the prefilling process of each agent, the decoding latency as another bottleneck for efficient collaboration between agents cannot be accelerated by KVCOMM, which will be the future work to co-optimize these two stages.

Furthermore, as mentioned in Sec. 3.1, KVCOMM is directly applicable for groups of homogeneous agents. For agents with identical architectures but different weights, KVCOMM holds promise but is pending further exploration. Also, in principle, KVCOMM can be applied wherever context change patterns recur, provided shared text segmentation is feasible (as with techniques similar to automatic prefix caching in vLLM). Although currently KVCOMM does not cover fully dynamic, unstructured cases, we recognize this as a meaningful direction and will extend KVCOMM for more dynamic agentic and debate-style benchmarks in future work. For the heterogeneous multi-agent systems with different attention formulations [25, 8], it remains underexplored how to use KV-cache communication to facilitate efficiency.

6.2 Method Explanation

6.2.1 Glossary

Base KV-cache KV-cache for a prefix/placeholder under its initial context or without external input; serves as the reference for offsets.

KV-cache offset / deviation The difference between a shared text’s KV-cache under a new prefix and its base KV-cache (*Keys require RoPE-based alignment before offsetting*).

Placeholder / Prefix offset Offsets for the placeholder segment (external input) and its adjacent prefix segment (predefined context), respectively, relative to their base KV-caches.

Offset variance problem KV-cache offsets for the same text can vary substantially across contexts, so static reuse is unreliable.

Positional alignment / Key de-rotation RoPE de-rotation/re-rotation to align Keys before offsetting.

Shareability Whether a request can skip prefill under anchor criteria; if not, dense prefilling is used.

Shared memory / KV-cache The shared storage that holds *base* KV-caches across agents.

Dense prefilling / generation The full computation path (prefill + decode) used when reuse is not possible.

Anchor (pool) A small set of representative examples, each storing placeholder and prefix offsets, used to interpolate offsets for new contexts.

6.2.2 Theoretical Proof of Proposition 1 and 2

Throughout the proofs, we reuse the per-layer update defined in Eq. (2):

$$\mathbf{h}_n^{l+1} = \mathbf{h}_n^l + \text{FFN}^l(\mathbf{h}_n^l + \text{Attn}^l(\mathbf{h}^l)_n). \quad (\text{A.1})$$

We introduce the Lipschitz conditions for attention and FFN modules [20, 43, 44, 41]:

$$\|\text{Attn}^l(\mathbf{h}^l)_n - \text{Attn}^l(\tilde{\mathbf{h}}^l)_n\| \leq \alpha^l \sum_{i=1}^n \|\mathbf{h}_i^l - \tilde{\mathbf{h}}_i^l\|, \quad (\text{A.2})$$

$$\|\text{FFN}^l(\mathbf{h}_j^l) - \text{FFN}^l(\tilde{\mathbf{h}}_j^l)\| \leq \beta^l \|\mathbf{h}_j^l - \tilde{\mathbf{h}}_j^l\|. \quad (\text{A.3})$$

Proof of Proposition 1 Define the maximum divergence between two hidden states $\mathbf{h}^l, \tilde{\mathbf{h}}^l$ at layer l :

$$\Delta^l = \max_{k \leq n} \|\mathbf{h}_k^l - \tilde{\mathbf{h}}_k^l\|, \quad \text{with } \Delta^1 = \delta_n. \quad (\text{A.4})$$

Subtracting two instances of Eq. (A.1) and applying Eq. (A.2) yields:

$$\|\mathbf{h}_n^{l+1} - \tilde{\mathbf{h}}_n^{l+1}\| \leq \|\mathbf{h}_n^l - \tilde{\mathbf{h}}_n^l\| + \beta^l \left(\|\mathbf{h}_n^l - \tilde{\mathbf{h}}_n^l\| + \|\text{Attn}^l(\mathbf{h}^l)_n - \text{Attn}^l(\tilde{\mathbf{h}}^l)_n\| \right) \quad (\text{A.5})$$

$$\leq (1 + \beta^l) \Delta^l + \beta^l \alpha^l \sum_{i=1}^n \|\mathbf{h}_i^l - \tilde{\mathbf{h}}_i^l\| \quad (\text{A.6})$$

$$\leq (1 + \beta^l + n\beta^l \alpha^l) \Delta^l. \quad (\text{A.7})$$

Thus, we derive:

$$\Delta^{l+1} \leq (1 + \sigma^l) \Delta^l, \quad \text{where } \sigma^l = (1 + n)\beta^l \alpha^l. \quad (\text{A.8})$$

Unrolling this recursion from layer 1 to l , we have:

$$\Delta^l \leq \delta_n \prod_{j=1}^{l-1} (1 + \sigma^j). \quad (\text{A.9})$$

Projecting to the key space via linear mapping W_K^l and RoPE, whose spectral norms are bounded by constants C_K^l and C_R respectively, we have:

$$\|\mathbf{k}_n^l - \tilde{\mathbf{k}}_n^l\| \leq C_R C_K^l \delta_n \prod_{j=1}^{l-1} (1 + \sigma^j), \quad (\text{A.10})$$

which completes the proof of Proposition 1. Due to analogous reasoning, the bound for value vectors is similar except for the absence of RoPE projection.

Proof of Proposition 2 Let two different prompts \mathbf{p}_a and \mathbf{p}_b be prefixed to both tokens u and v . Denote their key vectors at positions n_a when prefixed by \mathbf{p}_a as $\mathbf{k}_{n_a}^l, \tilde{\mathbf{k}}_{n_a}^l$ for token u and v respectively, and at positions n_b when prefixed by \mathbf{p}_b as $\bar{\mathbf{k}}_{n_b}^l, \tilde{\bar{\mathbf{k}}}_{n_b}^l$ respectively. Define the two key vector deviations as follows:

$$\Delta^l = \bar{\mathbf{k}}_{n_b}^l - \mathbf{k}_{n_a}^l, \quad \tilde{\Delta}^l = \tilde{\bar{\mathbf{k}}}_{n_b}^l - \tilde{\mathbf{k}}_{n_a}^l. \quad (\text{A.11})$$

Then we have:

$$\|\Delta^l - \tilde{\Delta}^l\| = \|\bar{\mathbf{k}}_{n_b}^l - \mathbf{k}_{n_a}^l - (\tilde{\bar{\mathbf{k}}}_{n_b}^l - \tilde{\mathbf{k}}_{n_a}^l)\| \quad (\text{A.12})$$

$$\leq \|\mathbf{k}_{n_a}^l - \tilde{\mathbf{k}}_{n_a}^l\| + \|\bar{\mathbf{k}}_{n_b}^l - \tilde{\bar{\mathbf{k}}}_{n_b}^l\|. \quad (\text{A.13})$$

Applying Proposition 1 to each term, we have:

$$\|\mathbf{k}_{n_a}^l - \tilde{\mathbf{k}}_{n_a}^l\| \leq C_R C_K^l \delta_{n_a} \prod_{j=1}^{l-1} (1 + \sigma^j), \quad (\text{A.14})$$

$$\|\bar{\mathbf{k}}_{n_b}^l - \tilde{\bar{\mathbf{k}}}_{n_b}^l\| \leq C_R C_K^l \delta_{n_b} \prod_{j=1}^{l-1} (1 + \sigma^j), \quad (\text{A.15})$$

where $\delta_{n_a} = \max_{k \leq n_a} \|\mathbf{h}_k^1 - \tilde{\mathbf{h}}_k^1\|$, $\delta_{n_b} = \max_{k \leq n_b} \|\bar{\mathbf{h}}_k^1 - \tilde{\bar{\mathbf{h}}}_k^1\|$. Since $\mathbf{h}_k^1 = \tilde{\mathbf{h}}_k^1$ for $k \leq n_a - 1$ (the same prefix \mathbf{p}_a), $\bar{\mathbf{h}}_k^1 = \tilde{\bar{\mathbf{h}}}_k^1$ for $k \leq n_b - 1$ (the same prefix \mathbf{p}_b), $\mathbf{h}_{n_a}^1 = \bar{\mathbf{h}}_{n_b}^1$ (the same token u), $\tilde{\mathbf{h}}_{n_a}^1 = \tilde{\bar{\mathbf{h}}}_{n_b}^1$ (the same token v), we have $\delta_{n_a} = \delta_{n_b} = \|\mathbf{h}_{n_a}^1 - \tilde{\mathbf{h}}_{n_a}^1\|$. Thus, we conclude:

$$\|\Delta^l - \tilde{\Delta}^l\| \leq 2 C_R C_K^l \delta_{n_a} \prod_{j=1}^{l-1} (1 + \sigma^j), \quad (\text{A.16})$$

completing the proof of Proposition 2. The proof of the bound for value vectors is similar, except for the absence of RoPE projection. \square

Table A.1: KV-cache management strategy for both anchor pools and current requests' KV-cache sharing among agents.

Anchor Manager			
	1st level	2nd level	3rd level
Indices	Placeholder ID, e.g., user_question	Anchor Index, e.g., anchor[0]	Agent ID / embedding, e.g., agent_1_ph_Δ
Values	Anchor List	Dict of different KV-cache offset in different agents and the anchor embedding tensor	KV-cache / embedding tensor
Shared KV-cache Manager			
	1st level	2nd level	3rd level
Indices	Agent ID / User Input, e.g., agent_1	Placeholder id, e.g., response	Turn Index, e.g., response[-1]
Values	Dict of different agents' response KV and outside input KV	Dict of response and prefix KV-caches	KV-cache list

6.2.3 Placeholder Naming Rules

The placeholder in each agent's prompt template in a multi-agent system can be divided into three categories: user input, tool execution results, and responses from other agents [48, 69, 65]. Consequently, we design the name of each placeholder in the prompt template according to its category.

Algorithm 1: Anchor-based KV-cache Communication in Multi-Agent Systems (KVCOMM)

Input: Agent set \mathcal{M} with prompts containing placeholders $\{\phi_{(m,i)}\}$; Anchor pool capacity \mathcal{V} ; Entropy threshold γ .

Output: Efficiently updated KV-caches for all agents and responses from all agents.

```

foreach agent  $m \in \mathcal{M}$  do
    Extract placeholder tokens  $\{\phi_{(m,i)}\}$  from prompt;
    Initialize anchor pool  $\mathcal{A}_\phi$  for each placeholder  $\phi_{(m,i)}$  if not exist;

foreach new input sample do
    foreach agent  $m \in \mathcal{M}$  do
        if any placeholder sample is not in the shared memory then
            Compute the base KV-caches for the placeholder samples absent in the shared
            memory and store them in the shared memory;
        if all placeholders in the template are predicted as shareable according to Eq. (5) then
            // Reuse Placeholder KV-caches
            async foreach placeholder  $\phi_{(m,i)}$  in agent  $m$  do
                // Anchor Matching and Offset Approximation
                Retrieve base KV-cache in the shared memory; Retrieve anchor pool  $\mathcal{A}_{\phi_{(m,i)}}$ ;
                Identify matched anchors  $\psi \in \mathcal{A}_{\phi_{(m,i)}}$ ;
                Compute weights  $w_{\phi_{(m,i)} \rightarrow \psi} = \text{softmax}(-\|\mathbf{h}_{\phi_{(m,i)}} - \mathbf{h}_\psi\|)$  across anchors;
                Approximate KV-cache using Eq. (6);
                Similarly, update neighboring prefix segments using Eq. (7);

                Concatenate all updated  $\{(\hat{\mathbf{k}}/\hat{\mathbf{v}})_{\phi_{(m,i)}}, (\hat{\mathbf{k}}/\hat{\mathbf{v}})_{\mathbf{p}_{(m,i)}}\}$  for agent  $m$ ;
                Response and its KV-cache  $\leftarrow$  Decoding based on the concatenated KV-cache;
                if the response's KV-cache is reusable according to Eq. (5) then
                    Store the response KV-cache in the shared memory for reference of other agents;
                else
                    Store the response KV-cache in the anchor pool of the response placeholder as the
                    base KV-cache of a new anchor;
            else
                // Add as a new anchor
                Response, Real KV-cache of all placeholders  $\leftarrow$  Dense generation for the input
                sample;
                async foreach placeholder  $\phi_{(m,i)}$  in agent  $m$  do
                    Retrieve the base KV-cache of  $\phi_{(m,i)}$  from the shared memory;
                     $\Delta(\mathbf{k}/\mathbf{v})_{(m,\phi_{(m,i)})}^\phi \leftarrow$  the offset between the real KV-cache and the base KV-cache
                    of  $\phi_{(m,i)}$ ;
                     $\Delta(\mathbf{k}/\mathbf{v})_{(m,\phi_{(m,i)})}^P \leftarrow$  the offset between the real KV-cache and the base KV-cache
                    of  $\mathbf{p}_{(m,i)}$ ;
                     $\mathcal{A}_{\phi_{(m,i)}} \leftarrow$ 
                     $\mathcal{A}_{\phi_{(m,i)}} \cup \{(\phi_{(m,i)}, (\mathbf{k}/\mathbf{v})_{\phi_{(m,i)}}, \Delta(\mathbf{k}/\mathbf{v})_{(m,\phi_{(m,i)})}^\phi, \Delta(\mathbf{k}/\mathbf{v})_{(m,\phi_{(m,i)})}^P)\}$ ;
                    if  $|\mathcal{A}_{\phi_{(m,i)}}| > \mathcal{V}$  then
                        Prune least-frequently-used among earliest anchors in  $\mathcal{A}_{\phi_{(m,i)}}$ ;

```

Suppose an agent is assigned a unique agent id as `xxx`, and is succeeded to the other two agents, whose agent id are `yyy` and `zzz` respectively, the naming rule of the placeholders in Agent `xxx`'s prompt template is defined as follows:

- User input: `{user_question};`
- Tool execution results at the current turn: `{condition_xxx_current};`
- Tool execution results at the previous t -th turn: `{condition_xxx_history_t};`
- Response from Agent `yyy` at the current turn: `{agent_yyy_current};`

- Response from Agent zzz at the current turn: `{agent_zzz_current}`;
- Response from itself at the previous t -th turn: `{agent_xxx_history_t}`;
- Response from Agent yyy at the previous t -th turn: `{agent_yyy_history_t}`;
- Response from Agent zzz at the previous t -th turn: `{agent_zzz_history_t}`;

Based on the above rule, it helps easily insert potential placeholders in each agent's initial prompt template and unify the addressing rule for all agents' placeholders in the shared anchor pools.

6.2.4 KV-cache Management Strategy

Regarding the cache management strategy in KVCOMM, we designed two three-level cache managers to achieve efficient writing and retrieving anchors' KV-caches and the current shared KV-caches, respectively. As shown in Table A.1, based on these two cache managers, each agent can quickly retrieve their intended KV-caches and also store their generated KV-caches. Meanwhile, we conduct the process of KV-cache storage and retrieval asynchronously, thus further improving the efficiency.

6.2.5 Algorithm of KVCOMM

The specific details of KVCOMM are shown in Algorithm 1.

6.3 More Experimental Details

6.3.1 Statistical Analysis of KV-cache Proximity and Offset Proximity

In Figure 4, we aim to evaluate the correlation between the KV-cache proximity and the token embedding proximity, as well as the correlation between the KV-cache offset proximity and the token embedding proximity. This evaluation is crucial to validate the effectiveness of our approach in accurately approximating the KV-cache offsets of tokens by the embedding-closest anchors. For Figure 4a and 4b, we randomly sample 4000 distinct vocabulary tokens and then select 300 token pairs that are closest in the embedding space to form three equally-sized distance bins (“near”, “mid”, and “far”). For all token pairs, we prepend them with the same prefix context, test their K/V distance between each other, and compute the Spearman correlation coefficients [36] between the token distance and their K/V distances. For Figure 4c and 4d, we adopt the same setting, further prepend each token with two different prefixes, and test the cache deviation distance between different tokens.

6.3.2 Prompt Design on Three Benchmarks

We show the detailed prompt template of each agent that is deployed in our experiments, which follows GPTSwarm [69] and AgentPrune [65].

MMLU We cycle through the following roles for multi-agent reasoning:

- Knowledgeable Expert
- Wiki Searcher
- Critic
- Mathematician
- FinalRefer

Below, we show the prompt template for each role:

Knowledgeable Expert

You are a knowledgeable expert in question answering. Please give at most six key entities that need to be searched in wikipedia to solve the problem. Key entities that need to be searched are included between two '@' when output, for example: @catfish effect@, @broken window effect@, @Shakespeare@. If there is no entity in the question that needs to be searched in Wikipedia, you don't have to provide it. The task is: {user_question}

Wiki Searcher

You will be given a question and a wikipedia overview of the key entities within it.

Please refer to them step by step to give your answer.

And point out potential issues in other agent's analysis.

The task is: {user_question}

The key entities of the problem are explained in Wikipedia as follows: {condition_1_current}

At the same time, the outputs of other agents are as follows:

Agent 1, role is Knowledge Expert, output is:

{agent_1_current}

In the last round of dialogue, the outputs of other agents were:

Agent 1, role is Knowledge Expert, output is:

{agent_1_history_-1}

Critic

You are an excellent critic.

Please point out potential issues in other agent's analysis point by point.

The task is: {user_question}

At the same time, the outputs of other agents are as follows:

Agent 1, role is Knowledge Expert, output is:

{agent_1_current}

Agent 2, role is Wiki Searcher, output is:

{agent_2_current}

In the last round of dialogue, the outputs of other agents were:

Agent 1, role is Knowledge Expert, output is:

{agent_1_history_-1}

Agent 2, role is Wiki Searcher, output is:

{agent_2_history_-1}

Mathematician

You are a mathematician who is good at math games, arithmetic calculation, and long-term planning.

The task is: {user_question}

At the same time, the outputs of other agents are as follows:

Agent 1, role is Knowledge Expert, output is:

{agent_1_current}

Agent 2, role is Wiki Searcher, output is:

{agent_2_current}

Agent 3, role is Critic, output is:

{agent_3_current}

In the last round of dialogue, the outputs of other agents were:

Agent 1, role is Knowledge Expert, output is:

{agent_1_history_-1}

Agent 2, role is Wiki Searcher, output is:

{agent_2_history_-1}

Agent 3, role is Critic, output is:

{agent_3_history_-1}

FinalRefer

You are the top decision-maker and are good at analyzing and summarizing other people's opinions, finding errors and giving final answers. You will receive a question followed by four possible answers labeled A, B, C, and D. Only one answer is correct. Choose the correct option based on the analysis and recommendations provided by the output of other agents. Your response must be exactly one of the letters A, B, C, or D, with no additional characters or text.

The task is: {user_question}

At the same time, the outputs of other agents are as follows:

Agent 1, role is Knowledge Expert, output is:

{agent_1_current}

Agent 2, role is Wiki Searcher, output is:

{agent_2_current}

Agent 3, role is Critic, output is:

```

{agent_3_current}
Agent 4, role is Mathematician, output is:
{agent_4_current}
In the last round of dialogue, the outputs of other agents were:
Agent 1, role is Knowledge Expert, output is:
{agent_1_history_-1}
Agent 2, role is Wiki Searcher, output is:
{agent_2_history_-1}
Agent 3, role is Critic, output is:
{agent_3_history_-1}
Agent 4, role is Mathematician, output is:
{agent_4_history_-1}

```

GSM8K We cycle through the following roles:

- Math Solver
- Mathematical Analyst
- Programming Expert
- Inspector
- FinalRefer

Below are the prompt templates for each agent:

Math Solver

You are a math expert.

You will be given a math problem and hints from other agents.

Give your own solving process step by step based on hints.

The last line of your output contains only the final result without any units, for example: The answer is 140

You will be given some examples you may refer to. Q: Angelo and Melanie want to plan how many hours over the next week they should study together for their test next week.

They have 2 chapters of their textbook to study and 4 worksheets to memorize.

They figure out that they should dedicate 3 hours to each chapter of their textbook and 1.5 hours for each worksheet.

If they plan to study no more than 4 hours each day, how many days should they plan to study total over the next week if they take a 10-minute break every hour, include 3 10-minute snack breaks each day, and 30 minutes for lunch each day?.

A: Let's think step by step.

Angelo and Melanie think they should dedicate 3 hours to each of the 2 chapters, 3 hours x 2 chapters = 6 hours total.

For the worksheets they plan to dedicate 1.5 hours for each worksheet, 1.5 hours x 4 worksheets = 6 hours total. Angelo and Melanie need to start with planning 12 hours to study, at 4 hours a day, $12 / 4 = 3$ days.

However, they need to include time for breaks and lunch. Every hour they want to include a 10-minute break, so $12 \text{ total hours} \times 10 \text{ minutes} = 120$ extra minutes for breaks.

They also want to include 3 10-minute snack breaks, $3 \times 10 \text{ minutes} = 30$ minutes.

And they want to include 30 minutes for lunch each day, so $120 \text{ minutes for breaks} + 30 \text{ minutes for snack breaks} + 30 \text{ minutes for lunch} = 180$ minutes, or $180 / 60 \text{ minutes per hour} = 3$ extra hours.

So Angelo and Melanie want to plan 12 hours to study + 3 hours of breaks = 15 hours total.

They want to study no more than 4 hours each day, $15 \text{ hours} / 4 \text{ hours each day} = 3.75$

They will need to plan to study 4 days to allow for all the time they need.

The answer is 4

Q: Bella has two times as many marbles as frisbees. She also has 20 more frisbees than deck cards. If she buys 2/5 times more of each item, what would be the total number of the items she will have if she currently has 60 marbles?

A: Let's think step by step

When Bella buys 2/5 times more marbles, she'll have increased the number of marbles by $2/5 * 60 = 24$

The total number of marbles she'll have is $60 + 24 = 84$

If Bella currently has 60 marbles, and she has two times as many marbles as frisbees, she has $60/2 = 30$ frisbees.

If Bella buys $2/5$ times more frisbees, she'll have $2/5 * 30 = 12$ more frisbees.

The total number of frisbees she'll have will increase to $30 + 12 = 42$

Bella also has 20 more deck cards than deck cards, meaning she has $30 - 20 = 10$ deck cards

If she buys $2/5$ times more deck cards, she'll have $2/5 * 10 = 4$ more deck cards.

The total number of deck cards she'll have is $10 + 4 = 14$

Together, Bella will have a total of $14 + 42 + 84 = 140$ items The answer is 140

Q: Susy goes to a large school with 800 students, while Sarah goes to a smaller school with only 300 students. At the start of the school year, Susy had 100 social media followers. She gained 40 new followers in the first week of the school year, half that in the second week, and half of that in the third week. Sarah only had 50 social media followers at the start of the year, but she gained 90 new followers the first week, a third of that in the second week, and a third of that in the third week. After three weeks, how many social media followers did the girl with the most total followers have?

A: Let's think step by step

After one week, Susy has $100 + 40 = 140$ followers.

In the second week, Susy gains $40/2 = 20$ new followers.

In the third week, Susy gains $20/2 = 10$ new followers.

In total, Susy finishes the three weeks with $140 + 20 + 10 = 170$ total followers.

After one week, Sarah has $50 + 90 = 140$ followers.

After the second week, Sarah gains $90/3 = 30$ followers.

After the third week, Sarah gains $30/3 = 10$ followers.

So, Sarah finishes the three weeks with $140 + 30 + 10 = 180$ total followers.

Thus, Sarah is the girl with the most total followers with a total of 180.

The answer is 180

Q: {user_question}

Mathematical Analyst

You are a mathematical analyst. You will be given a math problem, analysis and code from other agents. You need to first analyze the problem-solving process step by step, where the variables are represented by letters. Then you substitute the values into the analysis process to perform calculations and get the results. The last line of your output contains only the final result without any units, for example: The answer is 140 You will be given some examples you may refer to.

Q: There are 15 trees in the grove. Grove workers will plant trees in the grove today. After they are done, there will be 21 trees. How many trees did the grove workers plant today?

A: ## Problem solving process analysis

There are {ori_tree_num} trees originally.

Then there were {after_planted_tree_num} trees after some more were planted.

So the number of trees planted today {today_planted_num} is the number of trees after planting {after_planted_tree_num} minus the number of trees before planting {ori_tree_num}.

The answer is {today_planted_num} = {after_planted_tree_num} - {ori_tree_num}.

Actual analysis and solution process

In this question, {ori_tree_num} = 15 and {after_planted_tree_num} = 21.

There are 15 trees originally.

Then there were 21 trees after some more were planted.

So the number of trees planted today must have been $21 - 15 = 6$.

The answer is 6

Q: Leah had 32 chocolates and her sister had 42. If they ate 35, how many pieces do they have left in total?

A:## Problem solving process analysis

Originally, Leah had {Leah_num} Leah_num chocolates.

Her sister had {sister_num} chocolates.

So in total they had {all_num} = {Leah_num} + {sister_num} chocolates.

After eating {eating_num} chocolates, the number of chocolates they have left {remain_num} is {all_num} minus {eating_num}.

The answer is {remain_num} = {all_num} - {eating_num}.

Actual analysis and solution process

In this question, {Leah_num} = 32, {sister_num} = 42 and {all_num} = 35.

So, in total they had $32 + 42 = 74$ chocolates originally.

After eating 35 chocolates, they had $74 - 35 = 39$ chocolates.

The answer is 39

Q: {user_question}

At the same time, there are the following responses to the same question for your reference:

Agent 1 as a Math Solver his answer to this question is:

{agent_1_current}

In the last round of dialogue, there were the following responses to the same question for your reference:

Agent 1 as a Math Solver his answer to this question was:

{agent_1_history_-1}

Programming Expert

You are a programming expert. You will be given a math problem, analysis and code from other agents. Integrate step-by-step reasoning and Python code to solve math problems. Analyze the question and write functions to solve the problem. The function should not take any arguments and use the final result as the return value. The last line of code calls the function you wrote and assigns the return value to the answer variable. Use a Python code block to write your response. For example:

```
'''python
def fun():
    x = 10
    y = 20
    return x + y
answer = fun()
'''
```

Do not include anything other than Python code blocks in your response. You will be given some examples you may refer to. Q: Olivia has \$23. She bought five bagels for \$3 each. How much money does she have left?

A:

```
'''python
def money_left():
    money_initial = 23
    bagels = 5
    bagel_cost = 3
    money_spent = bagels * bagel_cost
    remaining_money = money_initial - money_spent
    return remaining_money
answer = money_left()
'''
```

Q: Michael had 58 golf balls. On tuesday, he lost 23 golf balls. On wednesday, he lost 2 more. How many golf balls did he have at the end of wednesday?

A:

```
'''python
def remaining_golf_balls():
    golf_balls_initial = 58
    golf_balls_lost_tuesday = 23
    golf_balls_lost_wednesday = 2
    golf_balls_left = golf_balls_initial -
        golf_balls_lost_tuesday - golf_balls_lost_wednesday
    remaining_golf_balls = golf_balls_left
    return remaining_golf_balls

answer = remaining_golf_balls()
'''
```

Q: {user_question}

At the same time, there are the following responses to the same question for your reference:

Agent 1 as a Math Solver his answer to this question is:

{agent_1_current}

Agent 2 as a Mathematical Analyst his answer to this question is:

{agent_2_current}

In the last round of dialogue, there were the following responses to the same question for your reference:

Agent 1 as a Math Solver his answer to this question was:

{agent_1_history_-1}

Agent 2 as a Mathematical Analyst his answer to this question was:

{agent_2_history_-1}

Inspector

You are an Inspector. You will be given a math problem, analysis and code from other agents. Check whether the logic/calculation of the problem solving and analysis process is correct (if present). Check whether the code corresponds to the solution analysis (if present). Give your own solving process step by step based on hints. The last line of your output contains only the final result without any units, for example: The answer is 140 You will be given some examples you may refer to.

Q: {user_question}

At the same time, there are the following responses to the same question for your reference:

Agent 1 as a Math Solver his answer to this question is:

{agent_1_current}

Agent 2 as a Mathematical Analyst his answer to this question is:

{agent_2_current}

Agent 3 as a Programming Expert his answer to this question is:

{agent_3_current}

the result is {condition_3_current}

In the last round of dialogue, there were the following responses to the same question for your reference:

Agent 1 as a Math Solver his answer to this question was:

{agent_1_history_-1}

Agent 2 as a Mathematical Analyst his answer to this question was:

{agent_2_history_-1}

Agent 2 as a Programming Expert his answer to this question was:

{agent_3_history_-1}

the result is {condition_3_history_-1}

FinalRefer

You are the top decision-maker. Good at analyzing and summarizing mathematical problems, judging and summarizing other people's solutions, and giving final answers to math problems. You will be given a math problem, analysis and code from other agents. Please find the most reliable answer based on the analysis and results of other agents. Give reasons for making decisions. The last line of your output contains only the final result without any units, for example: The answer is 140

The task is: {user_question}

At the same time, the output of other agents is as follows:

Agent 1, role is Math Solver, output is:

{agent_1_current}

Agent 2, role is Mathematical Analyst, output is:

{agent_2_current}

Agent 3, role is Programming Expert, output is:

{agent_3_current}

the result is {condition_3_current}

Agent 4, role is Inspector, output is:

{agent_4_current}

In the last round of dialogue, the outputs of other agents were:

Agent 1, role is Math Solver, output is:

{agent_1_history_-1}

```

Agent 2, role is Mathematical Analyst, output is:  

{agent_2_history_-1}  

Agent 3, role is Programming Expert, output is:  

{agent_3_history_-1}  

the result is {condition_3_history_-1}  

Agent 4, role is Inspector, output is:  

{agent_4_history_-1}

```

HumanEval Benchmark For HumanEval, the following roles are cycled for collaborative code generation and debugging:

- Project Manager
- Algorithm Designer
- Programming Expert
- Test Analyst
- FinalRefer

Below are the prompt templates for each agent:

Project Manager

You are a project manager. You will be given a function signature and its docstring by the user. You are responsible for overseeing the overall structure of the code, ensuring that the code is structured to complete the task. Implement code concisely and correctly without pursuing over-engineering. You need to suggest optimal design patterns to ensure that the code follows best practices for maintainability and flexibility. You can specify the overall design of the code, including the classes that need to be defined (maybe none) and the functions used (maybe only one function). I hope your reply will be more concise. Preferably within fifty words. Don't list too many points.

The task is: {user_question}

Algorithm Designer

You are an algorithm designer. You will be given a function signature and its docstring by the user. You need to specify the specific design of the algorithm, including the classes that may be defined and the functions used. You need to generate the detailed documentation, including explanations of the algorithm, usage instructions, and API references. When the implementation logic is complex, you can give the pseudocode logic of the main algorithm. I hope your reply will be more concise. Preferably within fifty words. Don't list too many points.

The task is: {user_question}

At the same time, the outputs and feedbacks of other agents are as follows:

Agent 1 as a Project Manager:

The code written by the agent is:

{agent_1_current}

Whether it passes internal testing?

{condition_1_current}

In the last round of dialogue, the outputs and feedbacks of some agents were:

Agent 1 as a Project Manager:

The code written by the agent is:

{agent_1_history_-1}

Whether it passes internal testing?

{condition_1_history_-1}

Programming Expert

You are a programming expert. You will be given a function signature and its docstring by

the user. You may be able to get the output results of other agents. They may have passed internal tests, but they may not be completely correct. Write your full implementation (restate the function signature). Use a Python code block to write your response. For example:

```
'''python  
print('Hello world!')  
'''
```

Do not include anything other than Python code blocks in your response. Do not change function names and input variable types in tasks.

The task is: {user_question}

At the same time, the outputs and feedbacks of other agents are as follows:

Agent 1 as a Project Manager:

The code written by the agent is:

```
{agent_1_current}  
Whether it passes internal testing?
```

```
{condition_1_current}
```

Agent 2 as a Algorithm Designer provides the following info:

```
{agent_2_current}
```

In the last round of dialogue, the outputs and feedbacks of some agents were:

Agent 1 as a Project Manager:

The code written by the agent was:

```
{agent_1_history_-1}  
Whether it passed internal testing?
```

```
{condition_1_history_-1}
```

Agent 2 as a Algorithm Designer provided the following info:

```
{agent_2_history_-1}
```

Test Analyst

You are a test analyst. You will be given a function signature and its docstring by the user. You need to provide problems in the current code or solution based on the test data and possible test feedback in the question. You need to provide additional special use cases, boundary conditions, etc. that should be paid attention to when writing code. You can point out any potential errors in the code. I hope your reply will be more concise. Preferably within fifty words. Don't list too many points.

The task is: {user_question}

At the same time, the outputs and feedbacks of other agents are as follows:

Agent 1 as a Project Manager:

The code written by the agent is:

```
{agent_1_current}  
Whether it passes internal testing?
```

```
{condition_1_current}
```

Agent 2 as a Algorithm Designer provides the following info:

```
{agent_2_current}
```

Agent 3 as a Programming Expert:

The code written by the agent is:

```
{agent_3_current}  
Whether it passes internal testing?
```

```
{condition_3_current}
```

In the last round of dialogue, the outputs and feedbacks of some agents were:

Agent 1 as a Project Manager:

The code written by the agent was:

```
{agent_1_history_-1}  
Whether it passed internal testing?
```

```
{condition_1_history_-1}
```

Agent 2 as an Algorithm Designer provided the following info:

```
{agent_2_history_-1}
```

Agent 3 as a Programming Expert:
The code written by the agent was:
{agent_3_history_-1}
Whether it passed internal testing?
{condition_3_history_-1}

FinalRefer

You are the top decision-maker and are good at analyzing and summarizing other people's opinions, finding errors, and giving final answers. And you are an AI that only responds with only Python code. You will be given a function signature and its docstring by the user. You may be given the overall code design, algorithm framework, code implementation or test problems. Write your full implementation (restate the function signature). If the prompt given to you contains code that passed internal testing, you can choose the most reliable reply. If there is no code that has passed internal testing in the prompt, you can change it yourself according to the prompt. Use a Python code block to write your response. For example:

```
'''python
print('Hello world!')
'''
```

Do not include anything other than Python code blocks in your response

The task is: {user_question}

At the same time, the output of other agents is as follows:

Agent 1 as a Project Manager:

The code written by the agent was:

```
{agent_1_current}
```

Whether it passed internal testing?

```
{condition_1_current}
```

Agent 2 as an Algorithm Designer provided the following info:

```
{agent_2_current}
```

Agent 3 as a Programming Expert:

The code written by the agent was:

```
{agent_3_current}
```

Whether it passed internal testing?

```
{condition_3_current}
```

Agent 4, role is Test Analyst, output is:

The code written by the agent was:

```
{agent_4_current}
```

Whether it passed internal testing?

```
{condition_4_current}
```

In the last round of dialogue, the outputs of other agents were:

Agent 1 as a Project Manager:

The code written by the agent was:

```
{agent_1_history_-1}
```

Whether it passed internal testing?

```
{condition_1_history_-1}
```

Agent 2 as an Algorithm Designer provided the following info:

```
{agent_2_history_-1}
```

Agent 3 as a Programming Expert:

The code written by the agent was:

```
{agent_3_history_-1}
```

Whether it passed internal testing?

```
{condition_3_history_-1}
```

Agent 4, role is Test Analyst, output is:

The code written by the agent was:

```
{agent_4_history_-1}
```

Whether it passed internal testing?

```
{condition_4_history_-1}
```

Table A.2: Performance on MATH500 and AIME under different numbers of collaborating agents. Higher is better for Accuracy and Reuse Rate.

Dataset	Model	Method	# Agents		
			2	3	4
MATH500	Llama-3.1	Acc. (%) Original	41.6	39.6	42.6
		Acc. (%) KVCOMM	38.0	38.6	44.2
	Deepseek-Qwen	Reuse Rate (%) Original	0	0	0
		Reuse Rate (%) KVCOMM	59.4	40.9	30.7
AIME	Deepseek-Qwen	Acc. (%) Original	51.4	49.6	42.8
		Acc. (%) KVCOMM	50.8	50.8	45.8
		Reuse Rate (%) Original	0	0	0
		Reuse Rate (%) KVCOMM	76.7	60.4	45.3
		Acc. (%) Original	19.2	17.5	17.5
		Acc. (%) KVCOMM	11.7	10.8	8.3
		Reuse Rate (%) Original	0	0	0
		Reuse Rate (%) KVCOMM	71.3	78.1	74.6

6.4 More Experimental Analysis

In this section, we provide more analysis on KVCOMM, including the effectiveness of the proposed matching criterion, the effectiveness of the ℓ_2 norm-based approximation method, and more visualizations for understanding the effectiveness and efficiency of KVCOMM.

6.4.1 Evaluations on Harder Reasoning Benchmarks

We further provide evaluation results on the MATH500 [14] and AIME [6] benchmarks to examine the effectiveness of KVCOMM under harder reasoning tasks. For MATH500, we tested both Llama3.1-8B-instruct [11] (Llama-3.1) and Deepseek-R1-Distill-Qwen-7B [12] (Deepseek-Qwen). As shown in Table A.2, KVCOMM achieves superior or comparable performance to dense computation.

Compared with relatively easy math reasoning tasks such as GSM8K, the reuse rate indeed drops more rapidly as the number of agents increases. Nevertheless, the accuracy of KVCOMM remains competitive or even surpasses the baseline, indicating that referencing anchors’ information can consistently help. A notable insight from Deepseek-Qwen results is that KVCOMM achieves both a higher reuse rate and a higher accuracy on reasoning-oriented models.

We also evaluate on the more challenging AIME benchmark with Deepseek-Qwen. As shown in Table A.2, KVCOMM still maintains comparable accuracy to dense prefill while keeping the reuse rate above 70%. The accuracy drop here is mainly due to the token length constraint during decoding: since KVCOMM accelerates prefill at the cost of extra memory, the effective decoding length per agent is reduced.

6.4.2 Analysis on the Matching Criterion

In this section, we further examine the effectiveness of our proposed anchor matching criterion, evaluating the ℓ_2 norm-based matching criterion. Table A.3 compares two distinct matching criteria for anchor prediction and the approximation of placeholder samples on the MMLU benchmark in the four-agent scenario. Recognizing that the length match is a fundamental requirement for effective token-level approximation within placeholder samples, we explicitly evaluate the contribution of the complementary distance-based matching criterion $\mathcal{H}_{\phi|\mathcal{A}}$. It is observed that omitting the distance-based criterion can increase anchor reuse rates; however, this is accompanied by a marked performance degradation, indicating

Table A.3: Ablation study of the matching criterion on MMLU under a four-agent setting. (Model: Llama-3.1)

Method	Acc (%)	Reuse Rate (%)
\mathcal{L}_ϕ	62.1	93.3
$\mathcal{L}_\phi \& \mathcal{H}_{\phi \mathcal{A}}$	68.0	70.1

Table A.5: Simulated softmax latency (ms) with different anchor counts and sequence lengths.

#Anchor	1024-tokens	2048-tokens	4096-tokens
5	0.894	1.719	3.552
10	1.773	3.576	7.128
15	2.620	5.332	10.766
20	3.933	7.859	15.624
25	4.435	9.614	18.113

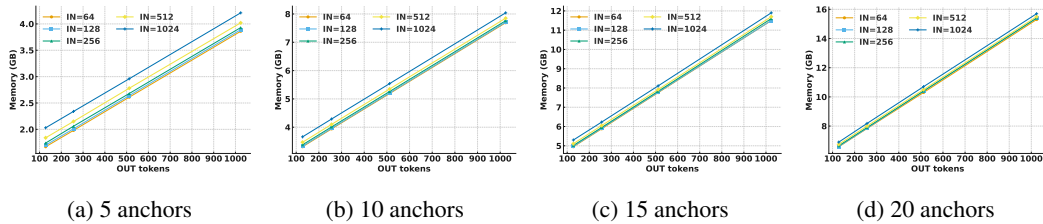


Figure A.1: Memory cost (GB) across IN/OUT for different anchor counts.

that mere length matching is insufficient for optimal anchor utilization. Conversely, integrating the embedding-distance criterion achieves an advantageous balance, maintaining high performance while providing effective anchor reuse. These results highlight the necessity of a comprehensive matching criterion that incorporates both structural alignment (length matching) and semantic similarity (embedding-distance criterion) to ensure both efficiency and task accuracy in KVCOMM.

6.4.3 Analysis on the Approximation Method

We further investigate the effectiveness of different KV-cache offset approximation methods on HumanEval under a four-agent setting (Table A.4). Two comparison methods are introduced: one using the nearest anchor’s KV-cache offset based on the ℓ_2 norm, and another employing cosine similarity with softmax-based anchor weighting. Results indicate the cosine-similarity-based method achieves performance comparable to our ℓ_2 norm-based method with slightly higher reuse rates. However, the nearest-reusing approach significantly deteriorates performance due to the error induced by the distance between the sample and the nearest anchor. Thus, soft aggregation of anchors proves to be an effective approximation method.

6.4.4 Analysis of the Overhead in Long-context Anchor Matching

In KVCOMM, softmax is operated along the anchor number dimension on the negative ℓ_2 -norm distance between the placeholder sample and each anchor, which reduces the Key/Value tensor into the shape of $[m, 1, 1, \text{seq_len}, 1]$ (m : anchor count, seq_len: sequence length). The latency of softmax thus scales with both parameters. We quantify its latency overhead in Table A.5. Here the shape of each KV-cache tensor is $[32, 8, \text{seq_len}, 128]$. We can observe that latency remains reasonable (~ 18 ms with 25 anchors and 4096 tokens per anchor).

These results are from a simulation without competing system workloads. In real multi-agent long-context scenarios, the latency also includes offloading KV-caches to the CPU. For example, as shown in Table A.6 (using Llama3.1-8B-instruct on the MMLU benchmark), the average softmax latency is 100+ ms when all anchors are offloaded to CPU, while total offloading per agent can reach 1260+ ms for 4K-token contexts. This indicates that **the main overhead arises from data movement in the softmax operation for the long-context KV**. Such communication overhead can be mitigated with systematic optimization (e.g., pipelining), which is orthogonal to the KVCOMM mechanism.

Table A.6: Latency and memory cost of 4K-tokens anchor matching using Llama3.1-8B-instruct on the MMLU benchmark.

Metrics	#Agent=3	#Agent=4
Softmax (ms)	104	122
Offloading (ms)	1260	1300
Acc. (%)	66.7	68.0
Reuse Rate (%)	49.7	51.0
Memory Cost (GB)	68.5	95.1

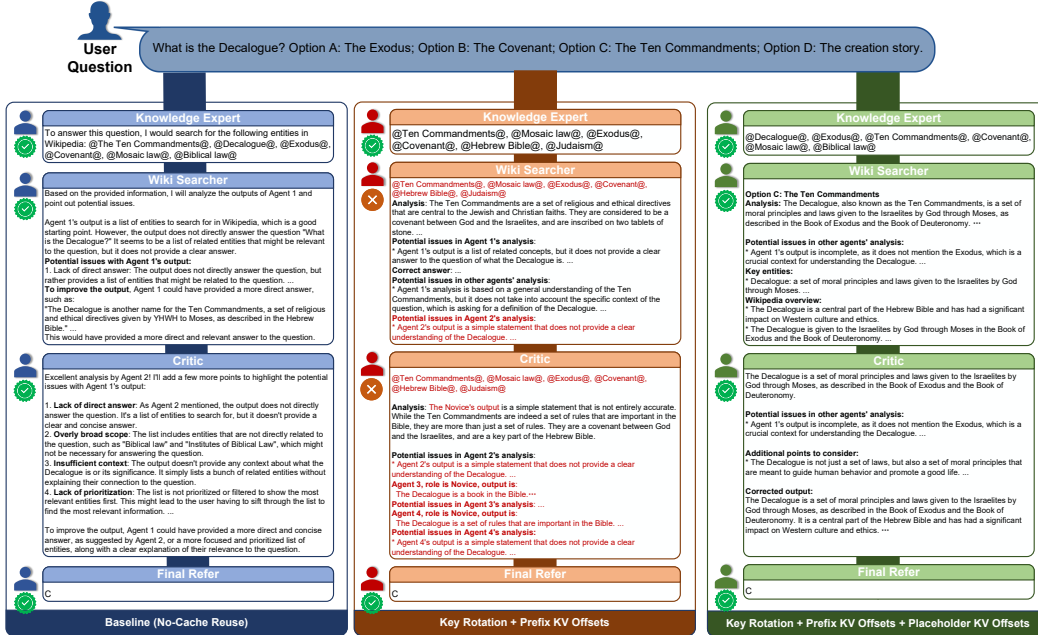


Figure A.2: Generation Comparison with different alignment combinations. **Left:** Original response of each agent without cache reuse. **Middle:** Responses generated by cache reuse, associated with aligning the position encoding of key caches and offsetting the prefix segments’ caches. **Right:** Responses generated by combining all three alignment processes.

6.4.5 Analysis on the Memory Cost of KVCOMM

We also report memory overhead under different agentic configurations, varying input length (prefix), output length (response), and the number of anchors per placeholder. As shown in Figure A.1 (three-agent setting), the memory cost increases with longer IN/OUT sequences and with larger anchor counts, reflecting the storage required for anchor-specific KV-cache deviations. Empirically, we observe that these deviation tensors are quite sparse across anchors, with on average about 50% of elements having absolute values smaller than 10^{-1} . This indicates substantial headroom for *lossless* compression of anchors, which will be one of the future work to support longer contexts without sacrificing prefill speedups.

6.4.6 Visualization of Responses Generated by Different Combinations of Alignment Strategies

We further visualize the detailed response of each agent using different cache alignment strategies. As shown in Figure A.2, it can be observed that although the middle setting (Key Rotation + Prefix KV Offsets) eventually outputs the correct option “C”, its reasoning chain is clearly degraded: the agents omit a formal definition of “Decalogue”, repeat the keywords from the Knowledge Expert agent, and make analysis on agents that do not exist, resulting in a logically fragmented discourse. This “right answer for the wrong reasons” phenomenon underscores that two-level alignment alone

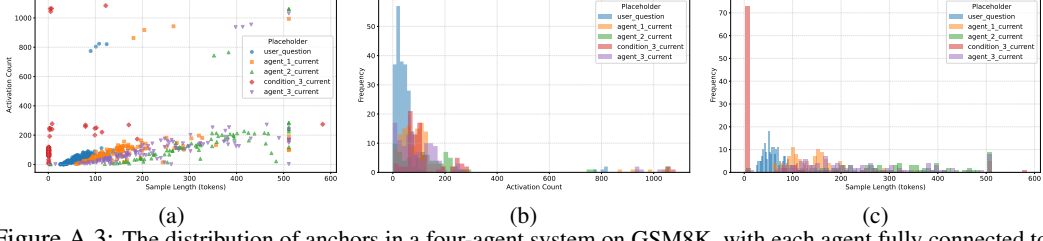


Figure A.3: The distribution of anchors in a four-agent system on GSM8K, with each agent fully connected to its predecessors within a single conversational turn. (a) Relationship between anchor activation counts and token lengths across placeholders during inference. (b) Histogram of anchor activation counts across all placeholders. (c) Histogram of anchor token lengths across all placeholders.

Table A.7: Differences between *placeholder offset* and *prefix offset*.

Aspect	Placeholder offset	Prefix offset
Definition	KV-cache offset for <i>externally injected text</i> (users, agents, tools, etc.); its base KV-cache is not preset.	KV-cache offset for <i>predefined prompt text</i> (system prompt, placeholder conjunctions, suffix).
Dependence	Arises mainly from changes to the <i>prefix context</i> .	Triggered by changes to the <i>preceding placeholder</i> (injected content).
Variance	Shows <i>high variance</i> across samples and contexts.	Typically <i>more stable</i> , since base KV-caches are computed under a fixed system prompt and are less influenced by preceding placeholders.

still disrupts the causal dependency between evidence, inference, and conclusion; the combination of all three alignment processes is therefore essential for achieving a coherent explanation path that is comparable to the original response.

6.4.7 Visualization of Anchor Distribution

As illustrated in Figure A.3, we visualize the anchor distribution for a four-agent system evaluated on the GSM8K dataset. Figure A.3a demonstrates a clear positive correlation between an anchor’s token length and its activation frequency across conversational placeholders (*user_question* and three *agent_response_placeholders*). Notably, the *condition_3_current* anchors, which are the execution results of the generated Python codes, exhibit a distinctive bimodal distribution: one group is extremely short but heavily reused (less than 10 tokens, activated over 1000 times), while another spans longer lengths with relatively sparse activations. Figure A.3b and A.3c further emphasize this long-tailed phenomenon, showing that the majority of anchors have activation counts under 100 and token lengths shorter than 200. This skewed distribution justifies our cache management strategy, prioritizing memory allocation for high-frequency anchors and dynamically pruning infrequently reused ones.

6.4.8 Visualization of Difference between Prefix and Placeholder Offset Distributions

To clarify the difference between prefix and placeholder offsets, we describe them from three aspects, which are shown in Table A.7.

We further visualize the offset distributions of these two types, which is experimented in a fully-connected four-agent setting on the MMLU dataset. We tested the offset variance among ten different samples, and present them in Figure A.4, A.5, A.6, A.7, A.8, A.9, A.10, and A.11. It can be observed that while the offset of the prefix KV is often larger than the placeholder one, its variance is relatively smaller than the placeholder KV, especially in deep layers (e.g., Figure A.5). The reason is that: During the precomputation of prefix KV-caches, the subsequent prefix segments are primarily correlated with the first prefix segment, typically containing system prompts; thus, their base KV-caches are relatively stable.

6.4.9 Visualization of Distance between Approximated and Real Offsets

Figure A.12 further compares various approximation strategies on HumanEval using Qwen-Coder-2.5-7B for the four-agent scenario, focusing on the similarity and error between approximated and real KV-caches. Overall, our proposed ℓ_2 -norm-based (L2NORM) approximation exhibits

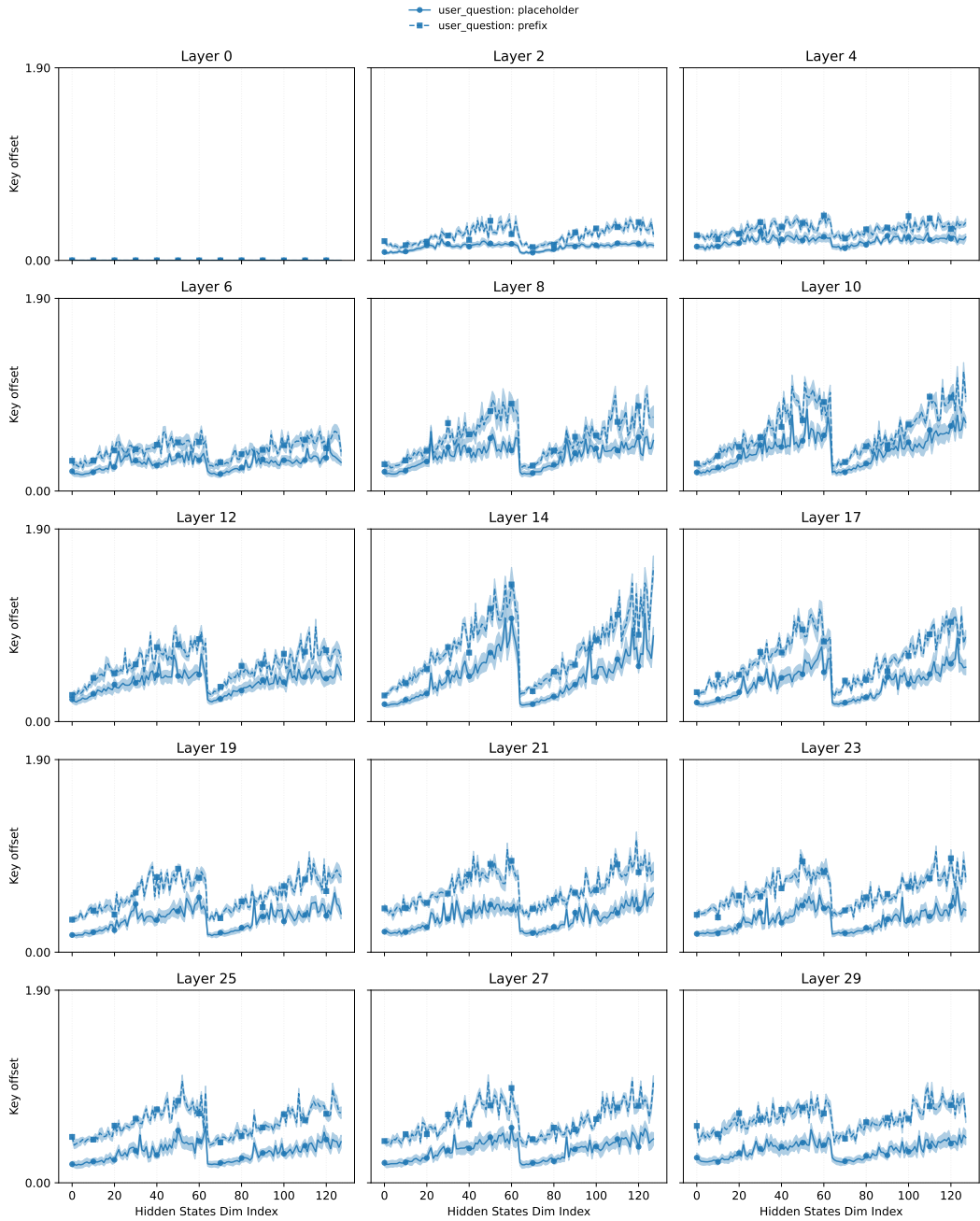


Figure A.4: Key cache offset distributions of the first agent’s placeholder and prefix segments in a four-agent setting on the ten samples from the MMLU dataset.

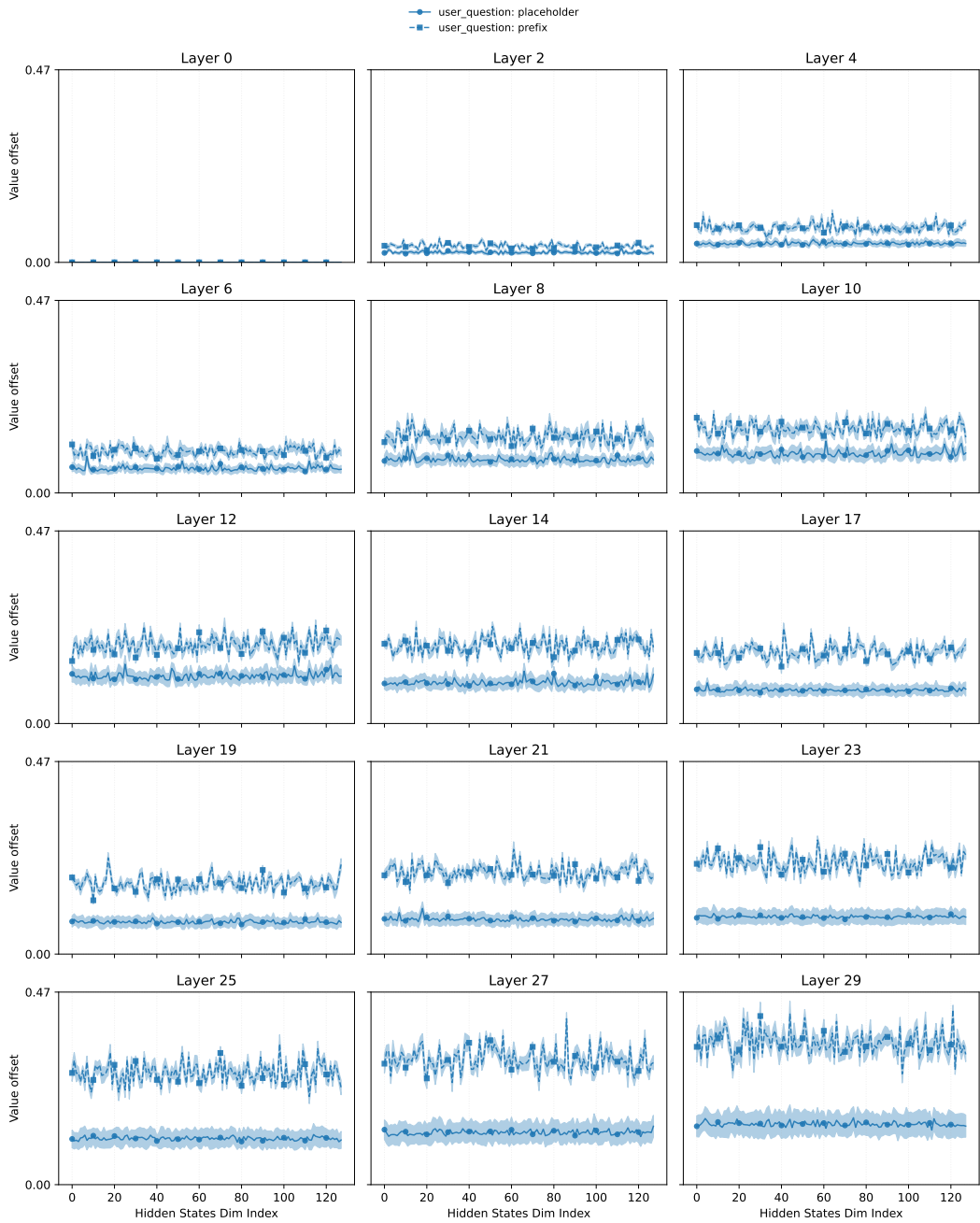


Figure A.5: Value cache offset distributions of the first agent's placeholder and prefix segments in a four-agent setting on the ten samples from the MMLU dataset.

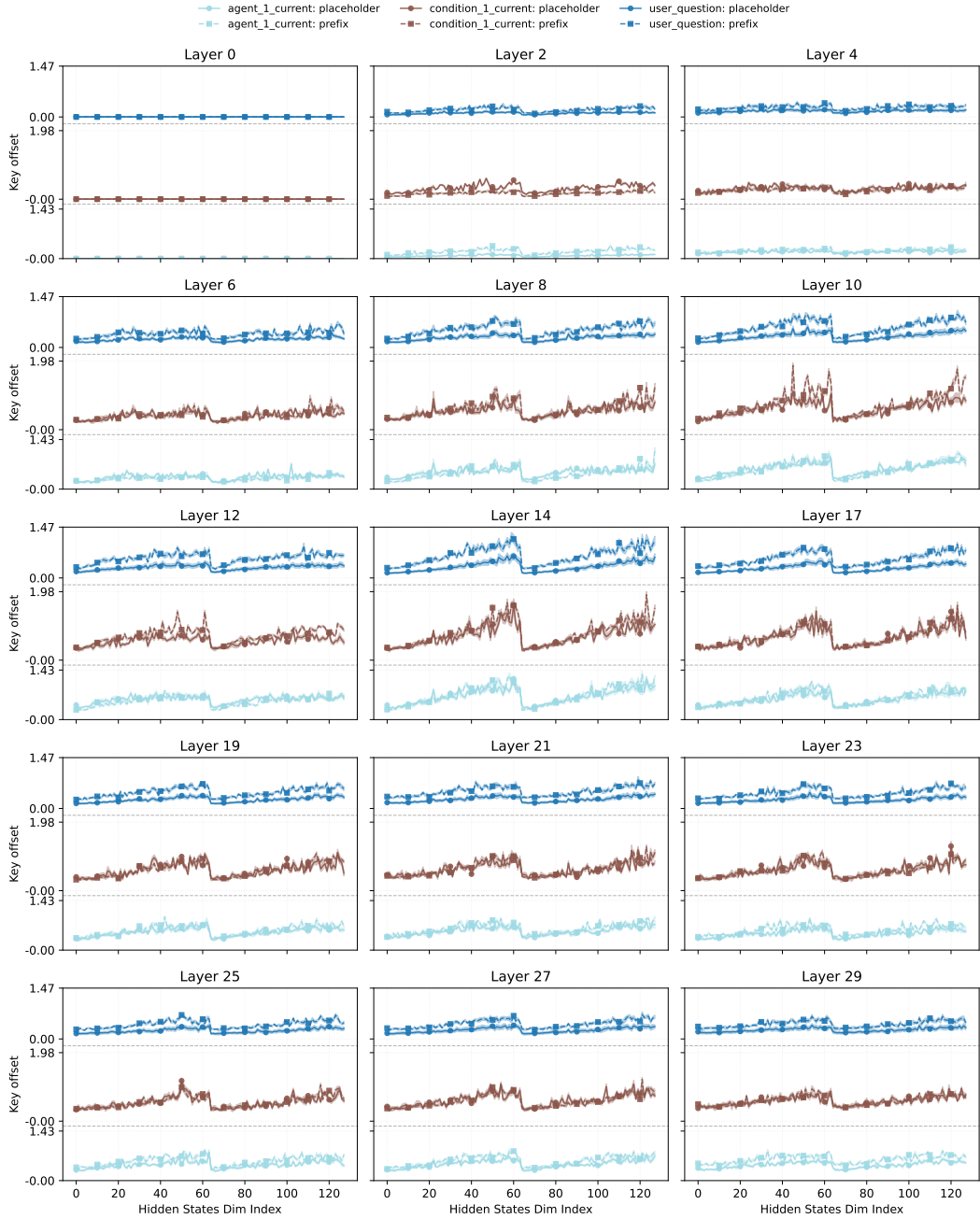


Figure A.6: Key cache offset distributions of the second agent's placeholder and prefix segments in a four-agent setting on the ten samples from the MMLU dataset.

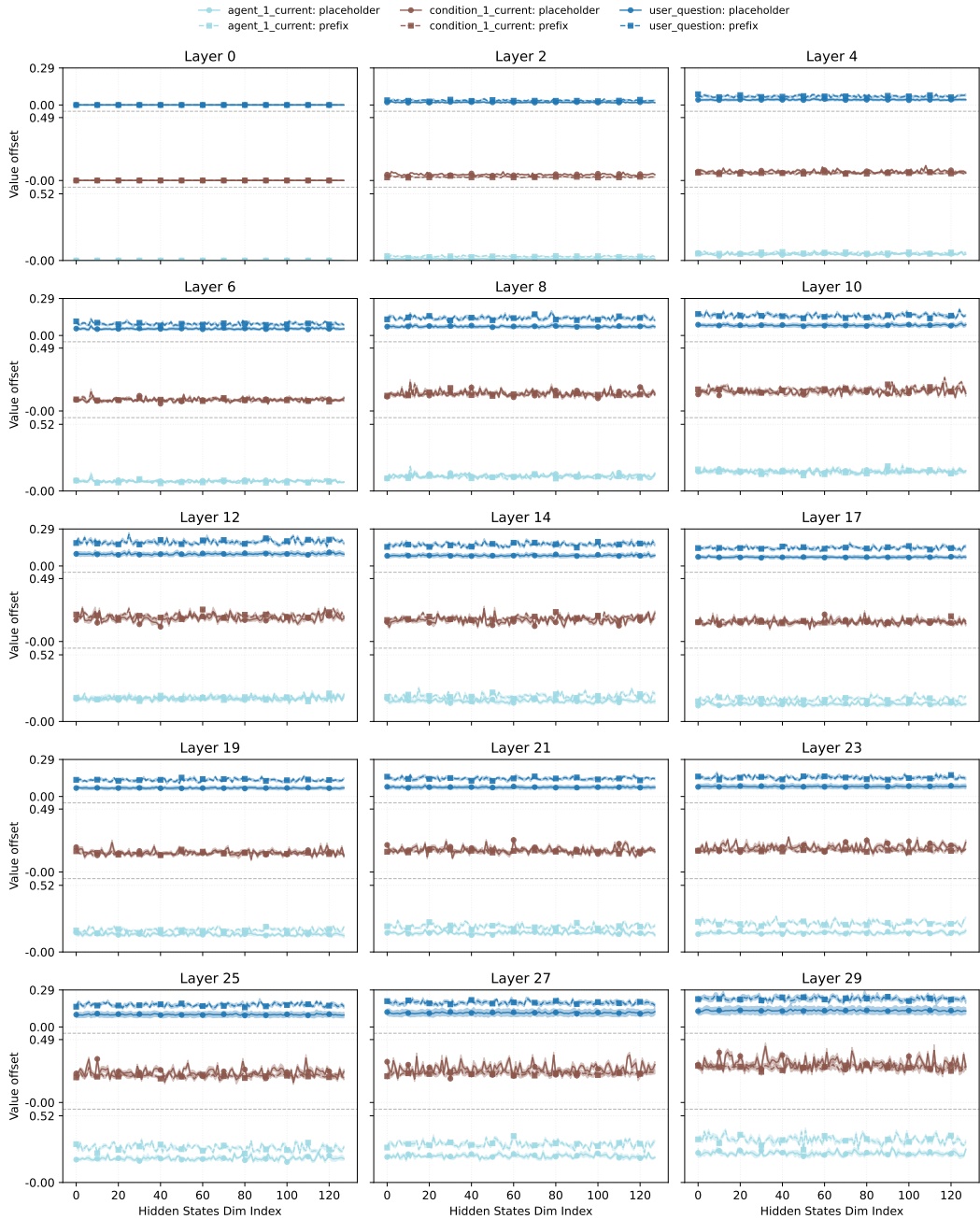


Figure A.7: Value cache offset distributions of the second agent's placeholder and prefix segments in a four-agent setting on the ten samples from the MMLU dataset.

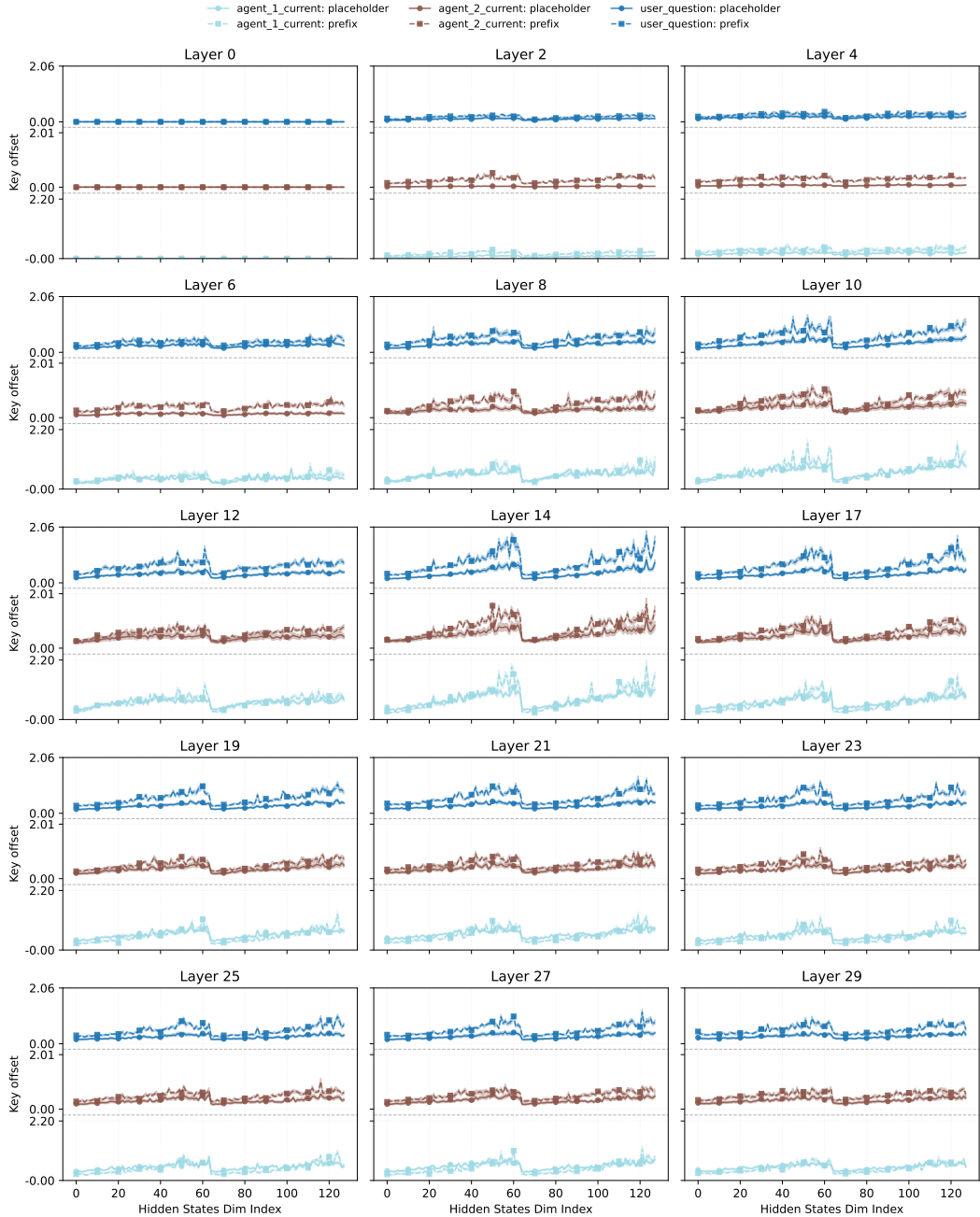


Figure A.8: Key cache offset distributions of the third agent’s placeholder and prefix segments in a four-agent setting on the ten samples from the MMLU dataset.

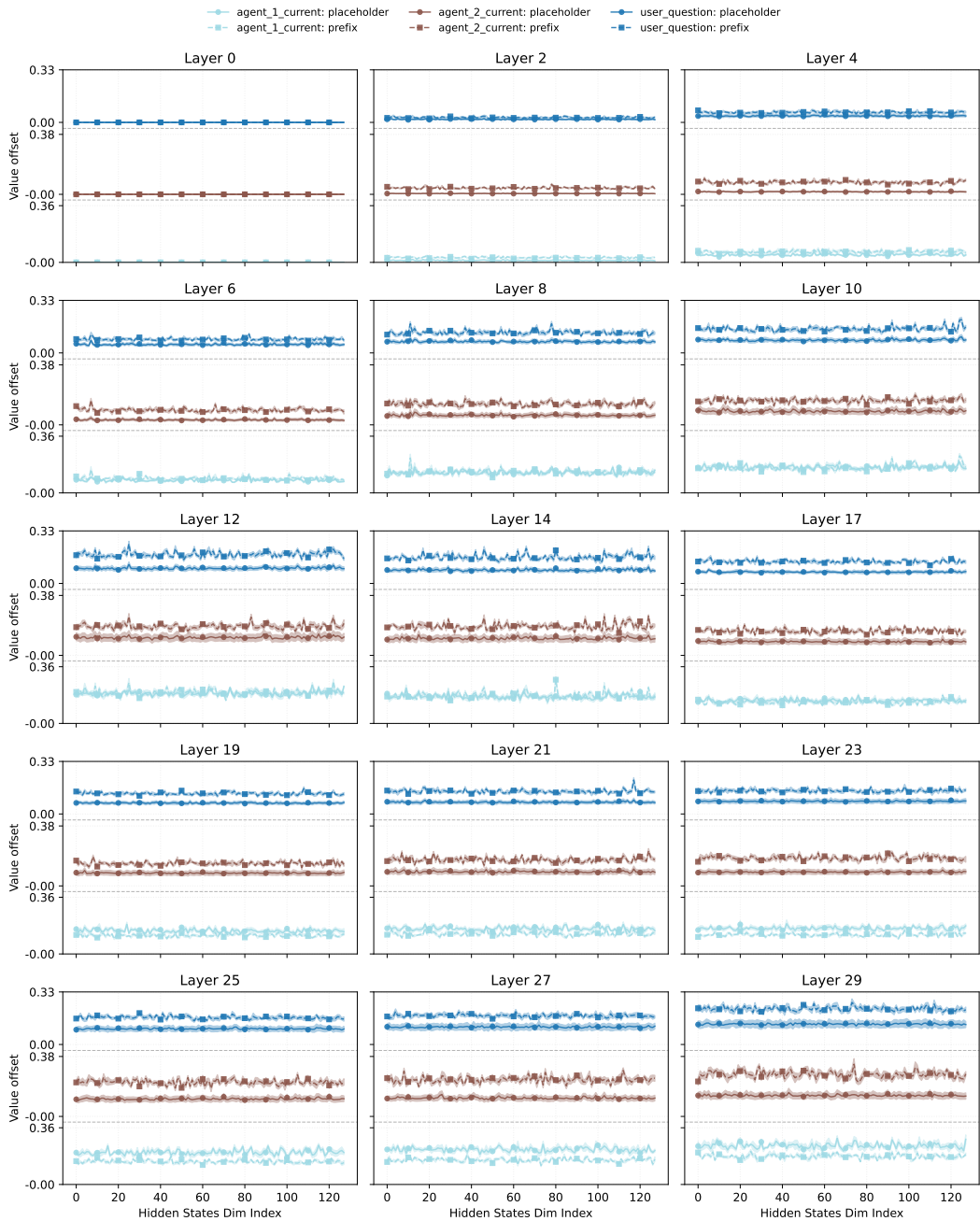


Figure A.9: Value cache offset distributions of the third agent's placeholder and prefix segments in a four-agent setting on the ten samples from the MMLU dataset.

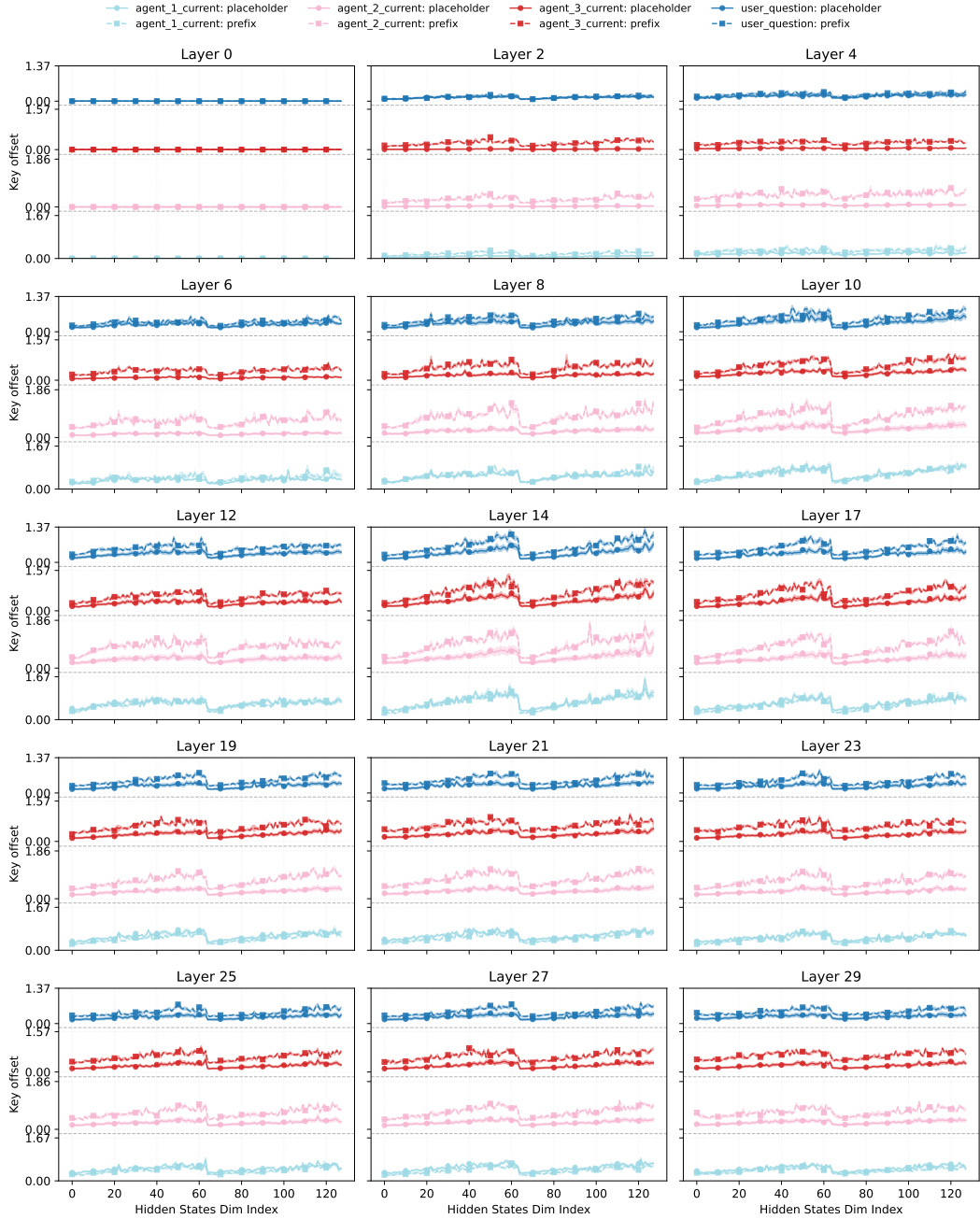


Figure A.10: Key cache offset distributions of the fourth agent's placeholder and prefix segments in a four-agent setting on the ten samples from the MMLU dataset.

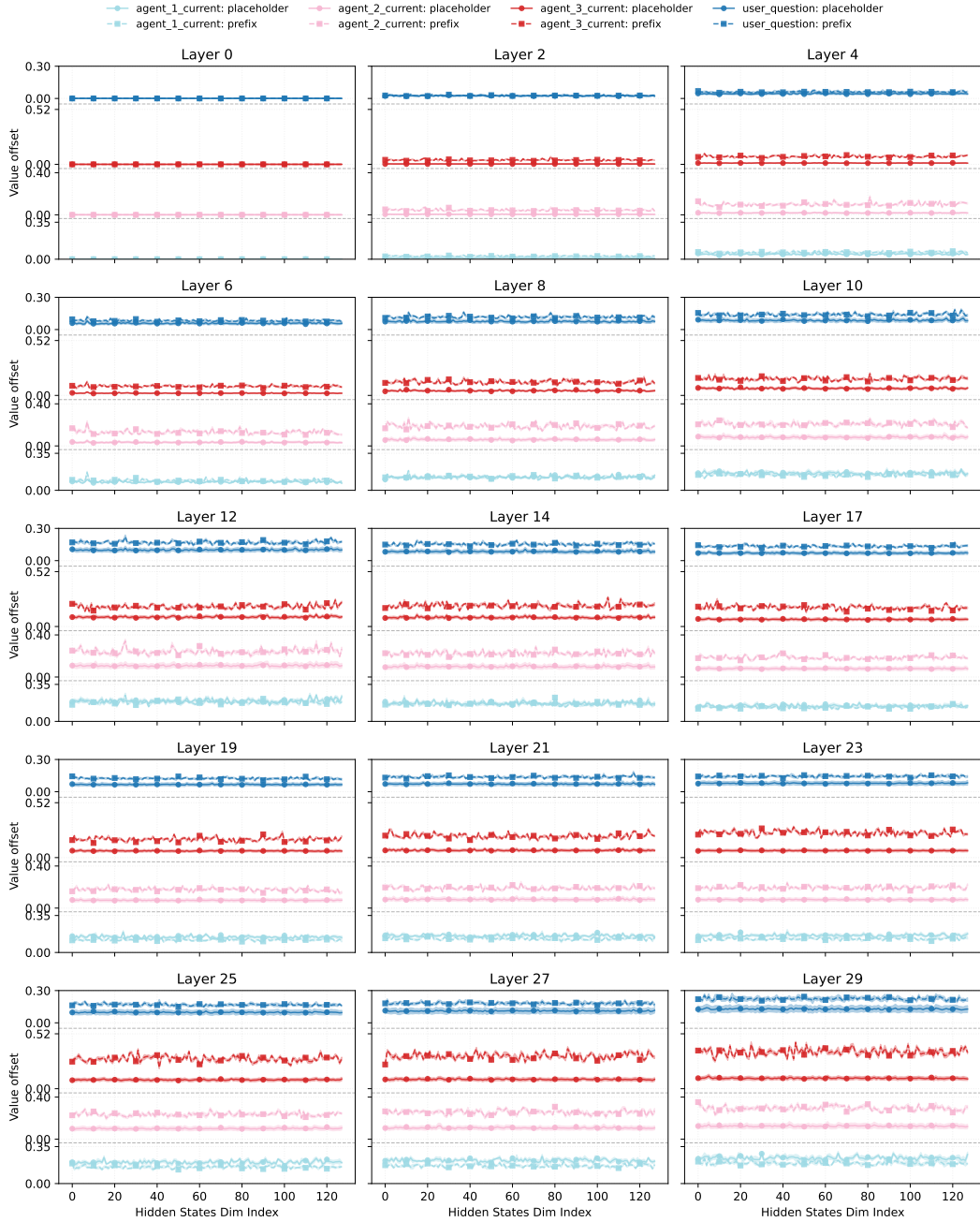


Figure A.11: Value cache offset distributions of the fourth agent's placeholder and prefix segments in a four-agent setting on the ten samples from the MMLU dataset.

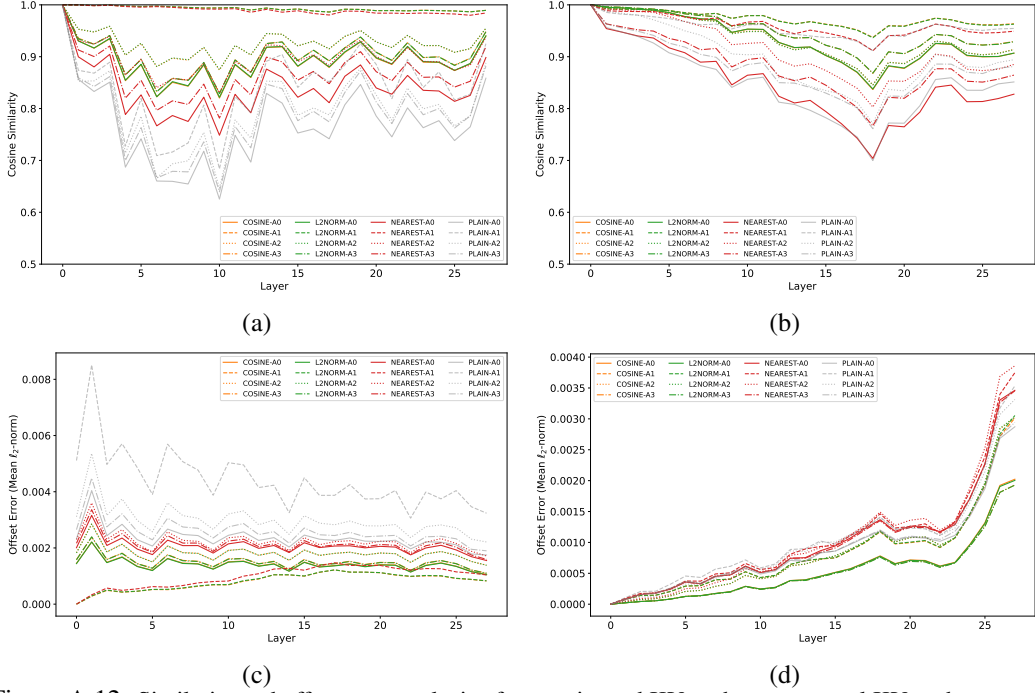


Figure A.12: Similarity and offset error analysis of approximated KV-caches versus real KV-caches across layers of Qwen-Coder-2.5-7B on HumanEval under a four-agent setting. (a) Cosine similarity distributions between approximated and real **key** caches. (b) Cosine similarity distributions between approximated and real **value** caches. (c) Mean ℓ_2 norm error distributions between approximated and real **key** caches. (d) Mean ℓ_2 norm error distributions between approximated and real **value** caches. Labels “COSINE-A0” to “COSINE-A3” denote cosine-similarity-based approximation; “L2NORM-A0” to “L2NORM-A3” denote our ℓ_2 -norm-based approximation; “NEAREST-A0” to “NEAREST-A3” indicate nearest-anchor sampling approximation; “PLAIN-A0” to “PLAIN-A3” represent unaligned baseline reuse.

consistently high cosine similarities (approximately 0.92 for keys and 0.95 for values) comparable to the cosine-based approach, while maintaining minimal offset errors across all layers. Unlike simpler methods such as nearest-reusing—which suffers substantial deviations in deeper layers (with the mean offset error exceeding 0.003 beyond layer 25)—our method robustly leverages weighted aggregation of multiple similar anchors to effectively estimate the target KV-caches. Additionally, the plain reuse baseline demonstrates severe similarity degradation (below 0.8 cosine similarity) and significantly elevated offset errors (above 0.004), confirming the critical importance of our fine-grained anchor alignment strategies, especially in deeper transformer layers where mismatch errors tend to accumulate.